https://doi.org/10.5194/amt-2020-122
Preprint. Discussion started: 29 June 2020

Atmospheric Measurement Techniques Discussions

Validation of the Sentinel-5 Precursor TROPOMI cloud data with Cloudnet, Aura OMI O_2-O_2, MODIS and Suomi-NPP VIIRS

Steven Compernolle[1], Athina Argyrouli[2,3], Ronny Lutz[3], Maarten Sneep[4], Jean-Christopher Lambert[1], Ann Mari Fjæraa[5], Daan Hubert[1], Arno Keppens[1], Diego Loyola[3], Ewan O'Connor[6,7], Fabian Romahn[3], Piet Stammes[4], Tijl Verhoelst[1], and Ping Wang[4]

[1]Royal Belgian Institute for Space Aeronomy (BIRA-IASB), Ringlaan 3, 1180 Uccle (Brussels), Belgium
[2]Technical University of Munich, TUM Department of Civil, Geo and Environmental Engineering, Chair of Remote Sensing Technology, Munich, Germany
[3]German Aerospace Center (DLR), Münchener Straße 20, 82234 Weßling, Germany
[4]Royal Netherlands Meteorological Institute (KNMI), Utrechtseweg 297, 3730 AE De Bilt, The Netherlands
[5]Norsk Institutt for Luftforskning (NILU), Instituttveien 18, 2007 Kjeller, Norway
[6]Finnish Meteorological Institute (FMI), Helsinki, Finland
[7]University of Reading, Whiteknights, PO Box 217, Reading, Berkshire, RG6 6AH, United Kingdom

Correspondence: Steven.Compernolle@aeronomie.be

Abstract. Accurate knowledge of cloud properties is essential to the measurement of atmospheric composition from space. In this work we assess the quality of the cloud data derived from Copernicus Sentinel-5 Precursor (S5P) TROPOMI radiance measurements: cloud top height and cloud optical thickness (retrieved with the S5P OCRA/ROCINN_CAL algorithm), cloud height (S5P OCRA/ROCINN_CRB and S5P FRESCO) and radiometric cloud fraction (all three algorithms). The analysis combines: (i) the examination of cloud maps for artificial geographical patterns, (ii) the comparison to other satellite cloud data (MODIS, NPP-VIIRS and OMI O_2-O_2), and (iii) ground-based validation with respect to correlative observations (2018-04-30 to 2020-02-27) from the CLOUDNET network of ceilometers, lidars and radars. Peculiar geographical patterns were identified, and will be mitigated in future releases of the cloud data products. Zonal mean latitudinal variation of S5P cloud properties are similar to that of other satellite data. S5P OCRA/ROCINN_CAL agrees well with NPP VIIRS cloud top height and cloud optical thickness, and with CLOUDNET cloud top height, especially for the low (mostly liquid) clouds. For the high clouds, S5P OCRA/ROCINN_CAL cloud top height is below the cloud top height of VIIRS and of CLOUDNET, while its cloud optical thickness is higher than that of VIIRS. S5P OCRA/ROCINN_CRB and S5P FRESCO cloud height are well below the CLOUDNET cloud mean height for the low clouds, but match on an average better with the CLOUDNET cloud mean height for the higher clouds. As opposed to S5P OCRA/ROCINN_CRB and S5P FRESCO, S5P OCRA/ROCINN_CAL is well able to match the lowest CTH mode of the CLOUDNET observations.

1 Introduction

Since decades the global distribution of atmospheric constituents has been monitored by ultraviolet/visible/near-infrared (UV/VIS/NIR) spectrometers measuring at the nadir of a satellite the radiance scattered by the Earth's atmosphere and reflected by its surface.

https://doi.org/10.5194/amt-2020-122
Preprint. Discussion started: 29 June 2020

Atmospheric Measurement Techniques Discussions

The multi-channel UV Backscatter instrument BUV started the monitoring of the ozone column and profile in 1970-1976, continued since 1978 with the SBUV(/2) series (McPeters et al., 2013), and further extended nowadays with the OMPS-nadir series aboard the Suomi-NPP and JPSS platforms. In the late 1980s first maps of tropospheric ozone were derived from UV satellite measurements of the total ozone column (Fishman et al., 1990). In 1995, the first UV/VIS/NIR hyperspectral spectrometer in space, ERS-2 GOME (Burrows et al., 1999), paved the way to satellite observations of other species besides ozone: nitrogen dioxide (NO_2), bromine monoxide (BrO), formaldehyde ($HCHO$), glyoxal ($CHOCHO$), sulfur dioxide (SO_2)... In 2002-2012 Envisat SCIAMACHY (Bovensmann et al., 1999) added to the GOME capabilities short-wave infrared (SWIR) channels enabling the detection of methane (CH_4), carbon monoxide (CO), and carbon dioxide (CO_2). Since, the GOME and SCIAMACHY UV/VIS/NIR data records have been extended by Aura OMI (Levelt et al., 2018) and by three GOME-2 instruments aboard EPS/MetOp-A/B/C meteorological platforms. In the framework of the EU Earth Observation programme Copernicus (Ingmann et al., 2012) they will be further extended beyond horizon 2040 by the Sentinel-4, Sentinel-5 and CO2M missions, with enhanced capabilities like unprecedented spatial resolution. As a gap filler between heritage satellites and the Sentinel-5 series, Sentinel-5 Precursor (S5P) was launched in October 2017 with the TROPOspheric Monitoring Instrument (TROPOMI, Veefkind et al. (2012)) aboard. Since April 2018 this UV/VIS/NIR/SWIR hyperspectral imaging spectrometer provides daily, high-resolution, global measurements of atmospheric gases related to air quality, ozone depletion, climate change, UV radiation, and volcanic hazards to aviation.

Atmospheric composition measurements from space can be affected by the presence of clouds. Clouds can not only mask underlying parts of the atmosphere, but they can also modify the radiative transfer of sunlight within and around the field-of-view of the instrument and increase the sensitivity to atmospheric constituents above and between clouds (e.g., Wang et al. (2008)). Therefore, all atmospheric composition data processors include a treatment of cloud interferences and S5P is no exception. The effect of clouds on atmospheric constituent retrievals depends mainly on the effective fractional cloud coverage of the field of view (or cloud fraction) and the cloud top height, but other parameters play a role like the cloud optical thickness, the albedo, their altitude distribution and their horizontal patterns. Since GOME, all UV/VIS nadir sounders with an exception for OMI include measurements of the oxygen A band around 760 nm, from which two independent cloud parameters can be retrieved (Schuessler et al., 2014) - in addition to cloud height, either cloud fraction (Stammes et al., 2008) or cloud optical thickness (Loyola et al., 2010). Additional parameters like the cloud fraction (when not derived from the O_2 A band observations) can be retrieved from UV spectral measurements or from broadband polarization monitoring devices (Loyola, 1998; Lutz et al., 2016). Its spectral range being limited to 500 nm, the effective cloud fraction and effective cloud pressure for OMI are retrieved using a DOAS (Differential Optical Absorption Spectroscopy) fit of the O_2-O_2 absorption feature around 477 nm (Acarreta et al., 2004; Veefkind et al., 2016).

The OCRA/ROCINN algorithms have a long-standing history and have already been applied to a set of operational instruments starting with GOME on ERS-2 (Loyola et al., 2010). A continuous development and the flexibility of OCRA/ROCINN allowed their easy adaptation to subsequent missions like SCIAMACHY on Envisat (Loyola, 2004) and the GOME-2 instruments on-board MetOp-A/B/C (Lutz et al., 2016). Recently, the algorithms have also been adapted to the EPIC instrument onboard the DSCOVR satellite, which is located at the Lagrangian point L1 (Molina García et al., 2018). Now being opera-

https://doi.org/10.5194/amt-2020-122
Preprint. Discussion started: 29 June 2020


Atmospheric Measurement Techniques Discussions

tional for TROPOMI on Sentinel-5 Precursor (Loyola et al., 2018), the OCRA/ROCINN cloud retrieval scheme will also be used operationally for the upcoming UVN instrument on Sentinel-4, the first mission of its kind for a geostationary view of air quality over Europe.

FRESCO (Fast Retrieval Scheme for Clouds from the O2 A-band) is a fast algorithm to retrieve cloud fraction and cloud height by fitting the spectral reflectance inside and outside the O2 A-band at 760 nm by a Lambertian cloud model. The FRESCO retrieval method has been applied to GOME, SCIAMACHY, GOME-2 and TROPOMI. The method with its refinements over the years, like inclusion of Rayleigh scattering and directional surface albedo, has been described by Koelemeijer et al. (2001), Wang et al. (2008, 2016). FRESCO data are mainly used to correct for the cloud effect in trace gas retrievals, and to filter clouds in trace gas and aerosol retrievals. FRESCO-S (FRESCO for Sentinel) has been implemented in the L2 processor of TROPOMI as a support product for KNMI and SRON level 2 products. Due to the increase in the spectral resolution in the TROPOMI instrument, the different spectral grid for each viewing direction, and small wavelength shifts introduced by inhomogeneous illumination of the spectral slit due to spatial variation of the brightness of the scene, some changes were introduced in the FRESCO-S algorithm. The spectral resolution of the reflectance database was increased to allow for interpolation of the database to the wavelengths of the observation, rather than the reverse which is used in FRESCO. Each viewing direction has its own reflectance database, to adjust to the different nominal wavelength grids and the variation of the instrument spectral response function.

The OMI instrument covers the UV and visible wavelength range (270–500 nm). This means that the oxygen A-band that is used by FRESCO is not available in the spectral range measured by OMI, and an alternative cloud retrieval algorithm is required. For OMI a cloud retrieval algorithm was developed that uses the O2–O2 collision induced absorption feature at 477 nm. This is done by using a cloud model that is very similar to the model used in FRESCO (Acarreta et al., 2004; Veefkind et al., 2016). The sensitivity of the O_2–O_2 cloud retrieval algorithm differs from FRESCO, because of the different wavelength range with a generally much lower surface albedo, especially over vegetated land, and a reduced sensitivity for (very) high clouds due to the reduced absorption at low pressures due to the density-squared nature of the absorption feature itself. Otherwise, both FRESCO and O_2–O_2 Cloud are expected to retrieve a height around the mid-level of the cloud (Sneep et al., 2008; Stammes et al., 2008).

The OCRA/ROCINN_CAL, S5P OCRA/ROCINN_CRB and S5P FRESCO cloud properties are input to several other S5P products: total and tropospheric ozone column, ozone profile, stratospheric, tropospheric and total NO_2 column, tropospheric HCHO column, total SO_2 column, aerosol layer height and CH_4 column (Fig. 1). Hence, given the central role of the S5P cloud products, their validation is key. In this work, a comprehensive validation is performed using ground-based data from CLOUDNET as well as cloud data from other satellites: NPP-VIIRS, OMI and MODIS.

Section 2 gives an overview of the different cloud data products discussed in this work, the cloud properties, the S5P mission requirements, and establishes terminology. In section 3 the different satellite and ground-based data sets are described in more detail. Section 4.1.1 discusses peculiar geographical patterns that can occur in the current version of the S5P cloud products, and how these are improved in to-be-released versions. The latitudinal variation of zonal means of cloud fraction and of cloud height of different satellite cloud products is compared in Section 4.2. Section 4.3 compares specifically cloud top height and

https://doi.org/10.5194/amt-2020-122
Preprint. Discussion started: 29 June 2020

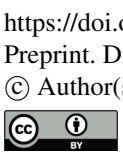

Atmospheric Measurement Techniques Discussions

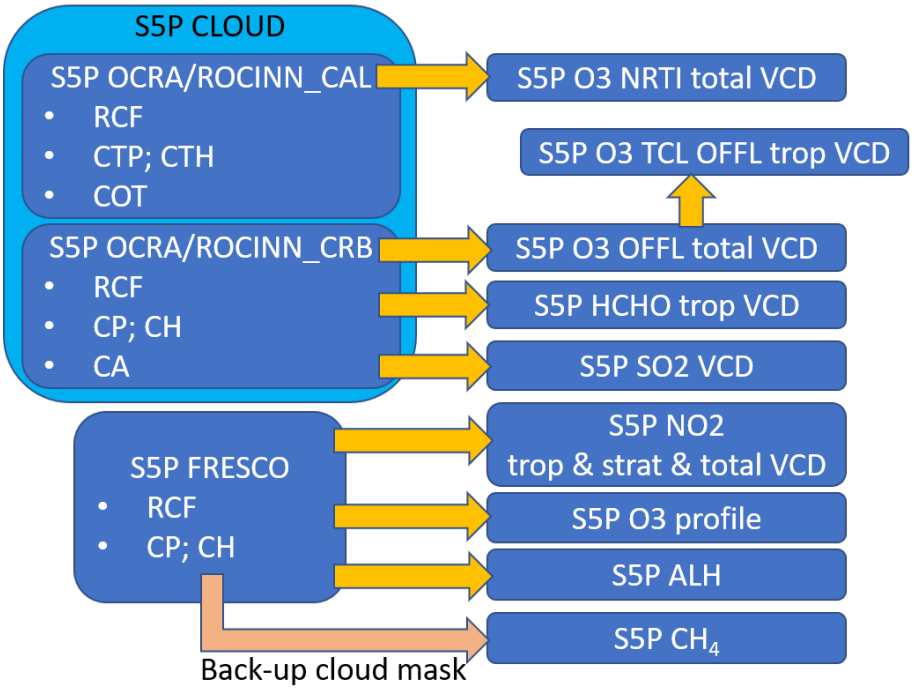

Figure 1. Flow chart indicating which S5P products use the cloud properties from S5P OCRA/ROCINN_CAL, S5P OCRA/ROCINN_CRB and S5P FRESCO. Note that S5P OCRA/ROCINN_CAL and S5P OCRA/ROCINN_CRB cloud properties are contained in the same S5P CLOUD product files. At the time of submission of this work, S5P O3 profile is not yet operational. Note that regarding to S5P CH_4, NPP-VIIRS is used as main cloud mask, while S5P FRESCO is merely a backup.

cloud optical thickness of S5P OCRA/ROCINN_CAL with those of NPP VIIRS (not the official production release but a prototype one). Cloud height of the S5P products is compared with ground-based CLOUDNET data in Section 4.4; here also a link is made to the OMI OMCLDO2 - CLOUDNET comparison. Finally, conclusions are given in Section 5.

2 Overview of cloud data products, properties, mission requirements and terminology

As we discuss here several cloud data products, with related but not always identical properties, some terminology conventions are in order. Table 1 contains an overview of properties discussed in this work (either as subject for validation or as important influence quantity) and the corresponding abbreviation and mathematical symbol. Table 2 contains an overview of cloud data products and main cloud properties.

The S5P CLOUD product files contain actually two subproducts: S5P OCRA/ROCINN_CAL and S5P OCRA/ROCINN_CRB. For both subproducts, a radiometric cloud fraction[1] (RCF; f_{rc}) is first obtained by the algorithm OCRA. The ROCINN_CAL

[1]The term 'effective cloud fraction' is sometimes also used in the literature (e.g., Stammes et al., 2008). Note that radiometric cloud fraction has to be clearly distinguished from the 'cloud radiance fraction' found in e.g., the S5P NO_2 data product and which is a different quantity.

https://doi.org/10.5194/amt-2020-122
Preprint. Discussion started: 29 June 2020

Atmospheric Measurement Techniques Discussions

Table 1. Properties, abbreviation and mathematical symbol.

Parameter	abbreviation	mathematical symbol
radiometric cloud fraction	RCF	f_{rc}
RCF, scaled to a fixed cloud albedo a	sRCF[b]	$f_{rc,a}$
geometrical cloud fraction[d]	GCF	f_{gc}
cloud top height & pressure	CTH, CTP	h_{ct}, p_{ct}
cloud height & pressure[a]	CH, CP	h_c, p_c
cloud optical thickness	COT	τ_c
cloud albedo	CA	A_c
surface albedo	SA	A_s
cloud mean height[c]	CMH	h_{cm}

a. These refer to the position of the optical centroid. See e.g., Stammes et al. (2008). This depends on the optical thickness of the cloud.
b. The relation between sRCF and RCF is $f_{rc,a} = f_{rc}A_c/a$. In this work always $a = 0.8$ is taken.
c. Calculated as the mean of the positions of the cloudy grid cells in a vertical cloud profile. This does not depend on cloud optical thickness.
d. GCF is not derived from S5P measurements.

algorithm retrieves a cloud top height (CTH; h_{ct}) and a cloud optical thickness (COT; τ_c). The ROCINN_CRB algorithm on the other hand retrieves a cloud height (CH; h_c) (which refers to the optical centroid of the cloud rather than to the cloud top) and a cloud albedo (CA; A_c). Note that a RCF is related to, but different from, a geometrical cloud fraction (GCF; f_{gc}) as provided by e.g., NPP/VIIRS and MODIS. In general RCF $\leq$ GCF; an example is a scene that is fully cloud covered ($f_{gc} = 1$) with an optically thin cloud ($f_{rc} < 1$) (Stammes et al., 2008).

Like S5P OCRA/ROCINN_CRB, S5P FRESCO retrieves an RCF and a CH referring to the optical center of the cloud, but an essential difference is that for most pixels, the CA is a fixed parameter equal to 0.8. The result is a scaled RCF (sRCF; $f_{rc,0.8}$), where $f_{rc,0.8} = f_{rc}A_c/0.8$. Also the OMCLDO2 algorithm provides an sRCF with CA fixed at 0.8 (Stammes et al., 2008). Therefore, when doing comparisons of (s)RCFs of products, we first convert all to an sRCF with CA fixed at 0.8. In the case of S5P OCRA/ROCINN_CRB, the cloud albedo A_c is attributed a fill value when the RCF $f_{rc} = 0$. Therefore, the conversion is done as follows

$$f_{rc,0.8} = f_{rc} * A_c/0.8, \text{ if } f_{rc} > 0 \qquad (1)$$
$$f_{rc,0.8} = 0, \text{ if} f_c = 0$$

Note that at maximum RCF and CA, sRCF reaches 1.2 rather than 1.

The OMCLDO2 data product contains a cloud pressure, but not a cloud height. Therefore, the cloud pressure is converted to a cloud height using a scale height of h_{scale} =7.668 km, (see Eq. (2))

$$h_c^{\text{OMCLDO2}} = -h_{\text{scale}} \ln\left(\frac{p_c}{p_s}\right) + h_s \qquad (2)$$

https://doi.org/10.5194/amt-2020-122
Preprint. Discussion started: 29 June 2020

Atmospheric Measurement Techniques Discussions

Table 2. Overview of cloud products, algorithms and main properties discussed in this work. The property abbreviations are explained in Table 1.

Product	Platform\sensor	Algorithm	Property
S5P OCRA/ROCINN_CAL[a]	S5P\TROPOMI	OCRA	RCF
		ROCINN_CAL	CTH, CTP, COT[b]
S5P OCRA/ROCINN_CRB[a]	S5P\TROPOMI	OCRA	RCF
		ROCINN_CRB	CH, CP, CA
S5P FRESCO	S5P\TROPOMI	FRESCO-S	sRCF[c], CP, CA
VIIRS	SNPP\VIIRS		GCF, CTP, COT
MODIS MYD08_D3[g]	Aqua\MODIS		GCF, CTP
OMCLDO2	Aura\OMI	OMCLDO2	sRCF[d], CH[e], CP
CLOUDNET	ground-based		CTH, CMH[f]

a. S5P OCRA/ROCINN_CAL and S5P OCRA/ROCINN_CRB subproducts are within the same S5P CLOUD product files.
b. Before comparing with VIIRS COT, the S5P OCRA/ROCINN_CAL is first converted to an *effective* COT using RCF×COT. More detail is provided in Section 4.3.
c. In S5P FRESCO, for most pixels, CA is fixed at 0.8. However, CA>0.8 is allowed to avoid cloud fractions larger than 1, so this is not strictly a sRCF. When doing actual comparisons between S5P FRESCO and other products, we therefore first convert to a strict sRCF with CA fixed at 0.8.
d. sRCF with CA fixed at 0.8.
e. CH is not provided as such in the OMCLDO2 product. It is calculated here using the OMCLDO2 CP and a scale height of 7.668 km, (see Eq. (2)).
f. CMH is not provided as such in the CLOUDNET product. We calculate it here considering classification labels 1-7 as cloudy grid cells and labels 0 and 8-10 as non-cloudy, following Veefkind et al. (2016).
g. Daily gridded L3 product, based on the L2 MYD06 product.

with p_s the surface pressure and h_s the surface altitude of the OMCLDO2 pixel. The value of 7.668 km was obtained by fitting to the AFGL Mid latitude summer (MLS) profile (Anderson et al., 1986), which is used as reference profile in the FRESCO algorithm.

The CLOUDNET classification data provides, among else, a CTH, which we use directly, and a classification of the vertical grid cells (classes 0 to 10, distinguishing e.g., clear sky, ice cloud, liquid cloud), which we convert to a vertical profile of cloudy (classes 1 to 7) and non cloudy (classes 0 and 8-10) following Veefkind et al. (2016). The cloud mean height (CMT; h_{cm}) is then calculated as the mean of the vertical positions of the cloudy grid cells.

More detail about the satellite data products and the cloud properties is provided in Section 3.

The mission requirements applicable to the cloud data product from the atmospheric composition Sentinels were first stated in ESA (2017a, b). Adapting the terminology[2] to be compliant with the international metrology standards VIM (International vocabulary of metrology) (JCGM, 2012) and GUM (Guide to the expression of uncertainty in measurement) (JCGM, 2008);

[2]In the ESA documentation 'bias' and 'random error' is used. The term 'random error' is not retained here as several components contribute to the uncertainty that are not random. Here we use the VIM/GUM terms bias (estimate of a systematic error) and uncertainty (non-negative parameter that characterizes the dispersion of the quantity values).

https://doi.org/10.5194/amt-2020-122
Preprint. Discussion started: 29 June 2020


Atmospheric Measurement Techniques Discussions

these are as follows: (i) the bias on cloud fraction, cloud height and cloud optical thickness may not exceed 20% and (ii) the uncertainty requirement is 0.05 for cloud fraction, 0.5 km for cloud height, and 10 for cloud optical thickness. We understand here that cloud fraction refers to the RCF (possibly scaled with a fixed cloud albedo), while cloud height can refer to both the cloud height at the optical centroid (as provided by S5P OCRA/ROCINN_CRB and S5P FRESCO) or the cloud top height (as provided by S5P OCRA/ROCINN_CAL). Since the beginning of its nominal operation in April 2018, in-flight compliance of S5p TROPOMI with these mission requirements has been monitored routinely by means of comparisons to ground-based reference measurements in the Validation Data Analysis Facility (VDAF) of the S5p Mission Performance Centre (MPC) and by confrontation with satellite data from MODIS, VIIRS and OMI.

Mission requirements relate to deviations of the satellite data from an (unknown) true value. But in comparisons with real-life reference data, deviations occur also due to imperfect reference measurements and moreover, because of different temporal/spatial/vertical sampling and smoothing properties (Loew et al., 2017). Frameworks and terminology related to comparisons are developed in Lambert et al. (2013); Verhoelst et al. (2015); Verhoelst and Lambert (2016); Keppens et al. (2019).

3 Description of the data sets

3.1 Satellite data sets

3.1.1 S5P TROPOMI CLOUD OCRA/ROCINN

The S5P CLOUD OCRA/ROCINN retrieval (Loyola et al., 2018) is a two-step algorithm where the OCRA (Optical Cloud Recognition Algorithm) computes the cloud fraction using a broad-band ultraviolet/visible (UV/VIS) color space approach and ROCINN (Retrieval of Cloud Information using Neural Networks) retrieves the cloud height, cloud optical thickness and cloud albedo from near-infrared (NIR) measurements in and around the oxygen A-band (760nm).

OCRA derives the cloud fraction from UV–VIS reflectances by separating the sensor measurements into two components: a cloud-free background and a remainder expressing the influence of clouds. A color-space approach is used, where broad-band UV-VIS reflectances are translated to blue and green colors. The underlying assumption is that clouds appear white in the color-space, meaning that the spectrum of a cloud is wavelength independent across the UV-VIS wavelength range. The actual radiometric cloud fraction is then determined as the distance between the fully cloudy "white" color and the clear-sky colors taken from the reflectance background composite maps. The cloud-free background consists of global monthly composite maps per color which are currently based on three years of OMI data. With the new S5P CLOUD version 2, these have been replaced based on TROPOMI data and the resolution was increased from 0.2 x 0.4 degrees to 0.1 x 0.1 degrees. In a pre-processing step, scan angle dependencies of the colors are addressed by fitting low-order polynomials to monthly mean reflectance data as a function of color, time, across-track pixel position (i.e. viewing zenith angle) and latitude. Instrumental degradation is currently not addressed in OCRA itself since the updated L1b data will themselves include a degradation correction.

ROCINN is a machine learning algorithm for retrieving two additional cloud parameters from the measured NIR radiances around the O2 A-band; the fitting window covers the full spectral range from 758 to 771 nm. The forward problem refers to

https://doi.org/10.5194/amt-2020-122
Preprint. Discussion started: 29 June 2020


Atmospheric Measurement Techniques Discussions

the simulation of sun-normalized radiances for different cloud configurations using the VLIDORT Radiative Transfer Model (RTM) (Spurr, 2006). A significant set of simulated radiances, which satisfies the conditions of the smart sampling (Loyola et al., 2016), is used for the training of the operational Neural Network (NN). The replacement of the exact RTM by a NN, which is a well tested approximation for complex operational algorithms like ROCINN, is in particular beneficial for gaining computational efficiency. The cloud top height and cloud albedo/optical thickness are the cloud parameters which can be retrieved simultaneously using Tikhonov regularization technique. Two cloud models are handled in ROCINN: (i) Clouds-as-Reflecting-Boundaries (CRB) which considers the cloud as a Lambertian reflector and (ii) Clouds-as-Layers (CAL) which considers the cloud as a homogeneous cluster of scattering liquid water spherical particles using Mie theory. The CAL cloud base height is not a retrieved quantity but it is fixed by assuming a constant cloud geometrical thickness of 1 km. Other complementary information about the surface properties have been initially estimated from a climatology. In the upcoming version 2 of the CLOUD processor, the geometry-dependent surface properties are retrieved directly from TROPOMI measurements within the ROCINN fitting window using the GE_LER algorithm (Loyola et al., 2020).

The nominal operational processing produces an offline (OFFL) data product, with the processor release that is active at the time. There have been a few reprocessing campaigns to produce a consistent data-set. The resulting RPRO files can be combined with OFFL data for longer time series. For the CLOUD product consolidated data produced with processor version 1.1.7 is available from 2018-04-30 (start of phase E2). Note that NRTI CLOUD uses the same processor as RPRO and OFFL, and therefore has nearly the same output (for the same processor version). For full technical details, the reader is referred to the Product Readme File (PRF), Product User Manual (PUM) and Algorithm Theoretical Basis Document (ATBD), all available at https://sentinels.copernicus.eu/web/sentinel/technical-guides/sentinel-5p/products-algorithms.

3.1.2 S5P TROPOMI FRESCO-S

FRESCO-S models a cloud as a Lambertian reflector, similar to S5P OCRA/ROCINN_CRB. FRESCO-S retrieves the information on cloud pressure p and effective cloud fraction c from the reflectance in and around the O_2 A band. FRESCO uses three about 1 nm wide wavelength windows, namely 758 – 759 nm (continuum, no absorption), 760 – 761 nm (strong absorption), and 765 – 766 nm (moderate absorption). So both retrieved parameters p and c are consistently retrieved from the same spectral region. As opposed to S5P OCRA/ROCINN_CRB, where cloud albedo is retrieved, in FRESCO-S, the cloud albedo is assumed to be 0.8, except when this assumption would lead to a cloud fraction larger than 1. In those cases the cloud fraction is set to 1, and the cloud albedo is fitted instead, but only if the cloud height is well separated from the surface. The FRESCO-S algorithm uses a surface albedo climatology based on GOME-2 (Tilstra et al., 2017). Due to the difference in overpass time between GOME-2 (in the morning) and Sentinel 5 precursor (in the afternoon), and the large discrepancy in the spatial resolution of both instruments the surface albedo climatology is currently considered as one of the larger sources of error for the FRESCO-S algorithm. To compensate, some adjustments are made to suppress negative effective cloud fraction due to a climatological surface albedo value that is higher than reality. Also note that for scenes with a surface albedo higher than the assumed cloud albedo, the cloud parameters are less reliable.

https://doi.org/10.5194/amt-2020-122
Preprint. Discussion started: 29 June 2020


Atmospheric Measurement Techniques Discussions

The version of FRESCO validated here is 1.3, with the same time range as for the S5P OCRA/ROCINN product. The FRESCO processing in all these versions is identical, as the changes only applied to other products. As this is a non-released support product, no official documentation is currently available for FRESCO-S. Information about earlier FRESCO algorithms can be found in Koelemeijer et al. (2001); Wang and Stammes (2014). Note that significant updates to the algorithm were introduced for Tropomi/Sentinel 5 precursor, to deal with the higher spectral resolution and the effects of spectral shifts on the input spectrum due to inhomogeneous slit illumination caused by partial cloud cover. Where in previous instruments (GOME, Sciamachy, GOME-2) the reflectance could be spectrally interpolated to the wavelength grid of the look-up table, for Tropomi we need to interpolate the look-up table to the wavelength grid of the observations. To make this possible, the look-up table is stored with a four-fold spectral oversampling so that spline interpolation can be used for this step.

From previous validation efforts we know that FRESCO retrieves a height near the optical extinction weighted mean height of the cloud, at least for scenes with a significant cloud cover. For scenes with clouds – or aerosols, the algorithm does not distinguish between the two – close to the surface, a height that is closer to the surface will be retrieved, in fact in many cases the actual surface height will be found. This defect can be remedied by using a wider window with low to moderate absorption in the O_2 A-band. Instead of 765 – 766 nm, a 5 nm wide window 765 – 770 nm will increase the sensitivity to low clouds. This new look-up table will be used for FRESCO versions 1.4 and later.

3.1.3 Suomi-NPP VIIRS

The Visible/Infrared Imager/Radiometer Suite (VIIRS) is one of the five instruments onboard the Suomi National Polar-orbiting Partnership (NPP) satellite platform launched at the end of October 2011. The spectral coverage expands from the visible (VIS) to infrared (IR) with 22 channels from 0.41 μm to 12.01 μm at two different spatial resolutions of 375 m and 750 m. Five channels are high-resolution image bands (I1-5 at 375m) and sixteen are moderate-resolution bands (M1-16 at 750m). The optical/microphysical property (i.e., CLDPROP_L2_VIIRS_SNPP) cloud product refers to the pixel resolution of 750m. This Level-2 (L2) product was developed by NASA (Platnick et al., 2017) to ensure continuity for the long-term records of Moderate Resolution Imaging Spectroradiometer (MODIS) and VIIRS heritages. Note that the VIIRS data used in this work are not part of NASA VIIRS production release files and potential differences cannot be ruled out. Within the CLDPROP algorithm, the cloud top properties are derived from NOAA's operational algorithms, the so-called Clouds from AVHRR Extended (CLAVR-x) processing system, in which the algorithm is based primarily on IR spectral channels, with the additional information of shortwave infrared (SWIR) channels. In particular, the cloud top height is derived from the AWG (Algorithm Working Group) Cloud Height Algorithm (ACHA) (Heidinger and Li, 2019; Heidinger et al., 2019). Moreover, the cloud optical and microphysical property product inherits the MOD06 cloud optical/microphysical property retrieval algorithm from Platnick et al. (2017). The cloud optical thickness COT is retrieved simultaneously with the cloud effective radius CER based on a two channel retrieval introduced in Nakajima and King (1990). Primarily the COT information is derived from the reflectance in a non-absorbing VIS, near infrared (NIR), or SWIR spectral channel which depends on the surface type. The CER information is provided by the reflectance in an absorbing SWIR or mid-wave infrared (MWIR).

https://doi.org/10.5194/amt-2020-122
Preprint. Discussion started: 29 June 2020


Atmospheric Measurement Techniques Discussions

3.1.4 MODIS

Moderate Resolution Imaging Spectroradiometer (MODIS) is on board of Terra and Aqua satellite in descending mode passing the equator in the morning from north to south and ascending mode passing from the equator in the afternoon from south to north, respectively. MODIS has 36 spectral bands ranging in wavelengths from 0.4 μm to 14.4 μm and data products are retrieved in three different spatial resolutions of 250 m, 500 m, and 1 km. The comparison with TROPOMI can be done for the ascending MODIS/Aqua and only in a daily basis using the level-3 MODIS gridded atmosphere daily global joint MYD08_D3 product (Platnick et al., 2015). It contains daily 1 x 1 degree grid average values of atmospheric parameters among others also cloud properties. Cloud-top temperature, height, effective emissivity, phase and cloud fraction are produced using infrared channels with 1-km-pixel resolution and stored in the level-2 MODIS cloud data product file MYD06_L2, which is one of the four level-2 MODIS atmosphere products used for the level-3 MODIS atmosphere daily global parameters.

3.1.5 Aura OMI OMCLDO2

The OMI OMCLDO2 product (Veefkind et al., 2009, 2016) is retrieved from level-1B VIS channel from the Dutch-Finnish UV-Vis nadir viewing spectrometer OMI (Ozone Monitoring Instrument) on NASA's EOS-Aura polar satellite. The nominal footprint of the OMI ground pixels is 24×13 km^2 (across $\times$ along track) at nadir to 165×13km^2 at the edges of the 2600 km swath, and the ascending node local time is 13:42 hrs. The OMCLDO2 cloud model is similar to the cloud model used in the FRESCO algorithm, with the difference that it is based on the O_2-O_2 collision-induced absorption rather than O2 absorption lines, as the O_2 A-band is not observed by OMI. As a result it is more sensitive to lower altitudes. Similar to FRESCO, it fixes the cloud albedo at 0.8, retrieves a radiometric cloud fraction and cloud height, and is sensitive not only to cloud but also to aerosol. The retrieved cloud height is more representative of cloud midheight rather than a cloud top height (Sneep et al., 2008).

Following Veefkind et al. (2016) we include here a comparison of OMCLDO2 with CLOUDNET data, to judge how this is different from the S5P comparisons with CLOUDNET, using the same comparison settings.

3.2 Ground-based data sets

3.2.1 CLOUDNET

Europe operates a network of ground-based cloud-profiling active remote sensing stations as part of the Aerosol, Clouds and Trace Gas Infrastructure Network (ACTRIS). These stations operate vertically-pointing cloud radar and lidar/ceilometer and use the Cloudnet processing scheme (Illingworth et al., 2007) for the continuous evaluation of cloud profile properties. The Cloudnet scheme combines the cloud radar and lidar measurements at a temporal resolution of 30 s and a vertical resolution of 30 m to create a target categorization product which diagnoses the presence or absence in each pixel of: aerosol, insects, drizzle, rain, liquid cloud droplets, supercooled liquid droplets, ice cloud particles, melting ice cloud particles. Note that multiple targets can be diagnosed within a single pixel.

https://doi.org/10.5194/amt-2020-122
Preprint. Discussion started: 29 June 2020

Atmospheric Measurement Techniques Discussions

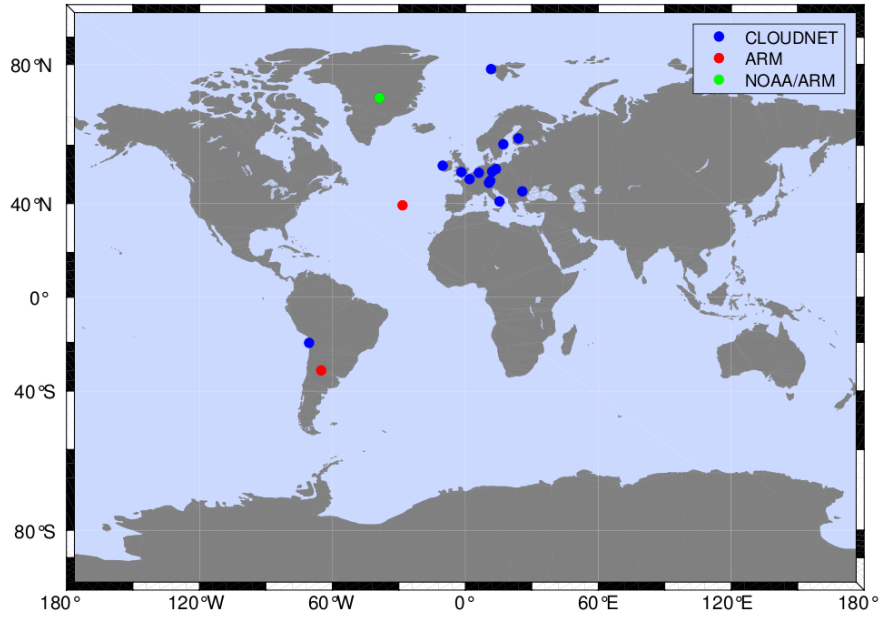

Figure 2. Selection of Cloudnet and ARM sites considered in this work.

The Cloudnet Level-2 classification product then takes the target categorization and simplifies the possible combinations into 9 main atmospheric target classifications at the same resolution (30 s and 30 m), together with the cloud base height and cloud top height. Following Veefkind et al. (2016), we consider target classification types 1-7 as cloud, and the remaining classification types as cloud-free.

The physical horizontal extent of the cloud radar measurements is on the order of 20 m at 1 km altitude, and 200 m at 10 km altitude, and much less for the lidar. Horizontal advection of clouds by the wind during the 30-s averaging time implies an effective horizontal extent that is usually larger than the physical horizontal extent; for example, a 30 $\mathrm{m\,s^{-1}}$ wind at 10 km yields an effective horizontal extent of 900 m for both instruments.

The Cloudnet processing scheme was also applied to similar cloud-profiling measurements from the US Department of Energy Atmospheric Radiation Measurement (ARM) sites. The sites included in this validation dataset are given in Table 3, displayed in Fig. 2, and Cloudnet products are freely available for download from the Cloudnet database (http://cloudnet.fmi.fi/).

4 Results

4.1 Geographical patterns

Global cloud maps of S5P OCRA/ROCINN and of S5P FRESCO were analyzed. Some peculiar patterns were discovered, described here below.

https://doi.org/10.5194/amt-2020-122
Preprint. Discussion started: 29 June 2020


Atmospheric Measurement Techniques Discussions

Table 3. Selection of Cloudnet and ARM sites considered in this work.

Station	lat[°],lon[°]	Location	Network
Ny-Alesund	78.93, 11.92	Svalbard	CLOUDNET
Summit	72.60, -38.42	Greenland	NOAA/ARM
Hyytiala	61.84, 24.29	Finland	CLOUDNET
Norunda	60.85, 17.48	Sweden	CLOUDNET
Mace Head	53.33, -9.90	Ireland	CLOUDNET
Lindenberg	52.21, 14.13	Germany	CLOUDNET
Leipzig	51.35,12.43	Germany	CLOUDNET
Chilbolton	51.14,-1.44	United Kingdom	CLOUDNET
Juelich	50.91, 6.41	Germany	CLOUDNET
Palaiseau	48.71, 2.21	France	CLOUDNET
Munich	48.15, 11.57	Germany	CLOUDNET
Schneefernerhaus	47.42, 10.98	Germany	CLOUDNET
Bucharest	44.35, 26.03	Romania	CLOUDNET
Potenza	40.60, 15.72	Italy	CLOUDNET
Graciosa	39.09, -28.03	Azores	ARM
Iquique	-20.54, -70.18	Chile	CLOUDNET
Villa Yacanto	-32.13, -64.73	Argentina	ARM

4.1.1 S5P OCRA/ROCINN

Geographical or swath related patterns may appear for some S5P OCRA/ROCINN parameters in S5P CLOUD version 1. Their appearance is not fully deterministic and is mainly related to the clear-sky background reflectance maps and scan-angle dependency correction that are both using OMI data in S5P CLOUD version 1. These OMI-based auxiliary data are functions of several parameters, e.g. time, wavelength, latitude, viewing zenith angle etc. The patterns listed below are not a general issue seen at all times and geolocations but rarely appear only for some combinations of (time, geometry, geolocation). With the update to CLOUD version 2, these OMI-based auxiliary data are replaced based on the TROPOMI data themselves and the effects listed below are largely reduced.

The following patterns may appear in S5P CLOUD version 1:

- an enhanced radiometric cloud fraction and cloud height mainly at the east edge of the swath at some months at some latitudes. Most pronounced effects seem to appear in the bands [40,60]°N and [30,40]°S. Figure 3 illustrates the issue for an example in the cloud top height in S5P CLOUD version 1 and the improvement in S5P CLOUD version 2, while Fig. S1 shows the issue for an example in the cloud fraction.

- A gradient in the cloud albedo with higher values in the northern hemisphere compared to the southern hemisphere (Fig. S2).

https://doi.org/10.5194/amt-2020-122
Preprint. Discussion started: 29 June 2020

Atmospheric Measurement Techniques Discussions

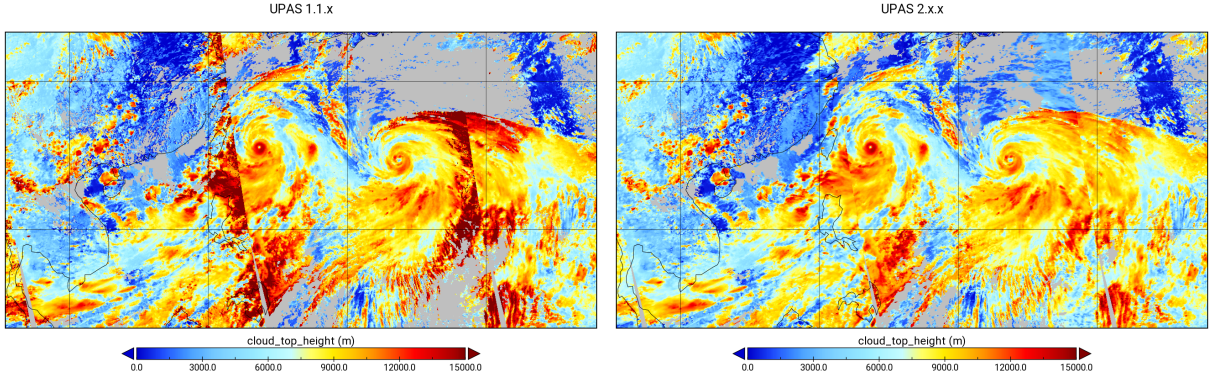

Figure 3. S5P OCRA/ROCINN_CAL CTH of parts of orbits 09416, 09417, 09418 on 2019-08-08 for the currently operational product CLOUD OFFL 1.1.7 (left) and the to-be-released CLOUD version 2 (right). Note the sharper contrast in CTH at an orbit edge for the released version.

4.1.2 S5P FRESCO

An issue in S5P FRESCO is that, at low radiometric cloud fraction, there is a tendency to retrieve a cloud height equal to the surface altitude. As an example, we discuss here a cloud-aerosol event captured by TROPOMI over China at 2019-02-23 (Fig. 4 and Fig. S3). The aerosol is observed by the S5P Absorbing Aerosol Index (AAI) product (Fig. 4, top left), and attributed a height of 300 to 500 m above the surface by the S5P Aerosol Layer Height (ALH) product (Fig. S3, bottom right). A low RCF cloud (RCF~0.3) of approximately the same shape is perceived by S5P FRESCO (Fig. 4, top right). Although a cloud is detected by S5P FRESCO, it is attributed zero offset from the surface (Fig. 4, bottom left).

A new version of S5P FRESCO, with a more wide fit window ('FRESCO-A wide') has been tested and is scheduled for release (S5P FRESCO version 1.4) in the near future. For this new product, the sensitivity to low clouds in the low atmosphere is improved. Fig. 4, bottom right, shows that FRESCO-A wide places the cloud at 300-500 m above the surface. Note the different horizontal extent of the cloud as perceived by FRESCO wide.

Errors in the cloud height can have an important impact on the retrieval of tropospheric NO_2 columns by TROPOMI. The improvement in NO_2 column retrieval by using FRESCO-A wide instead of the operational FRESCO version is discussed in more detail by Eskes et al. (2020).

https://doi.org/10.5194/amt-2020-122
Preprint. Discussion started: 29 June 2020

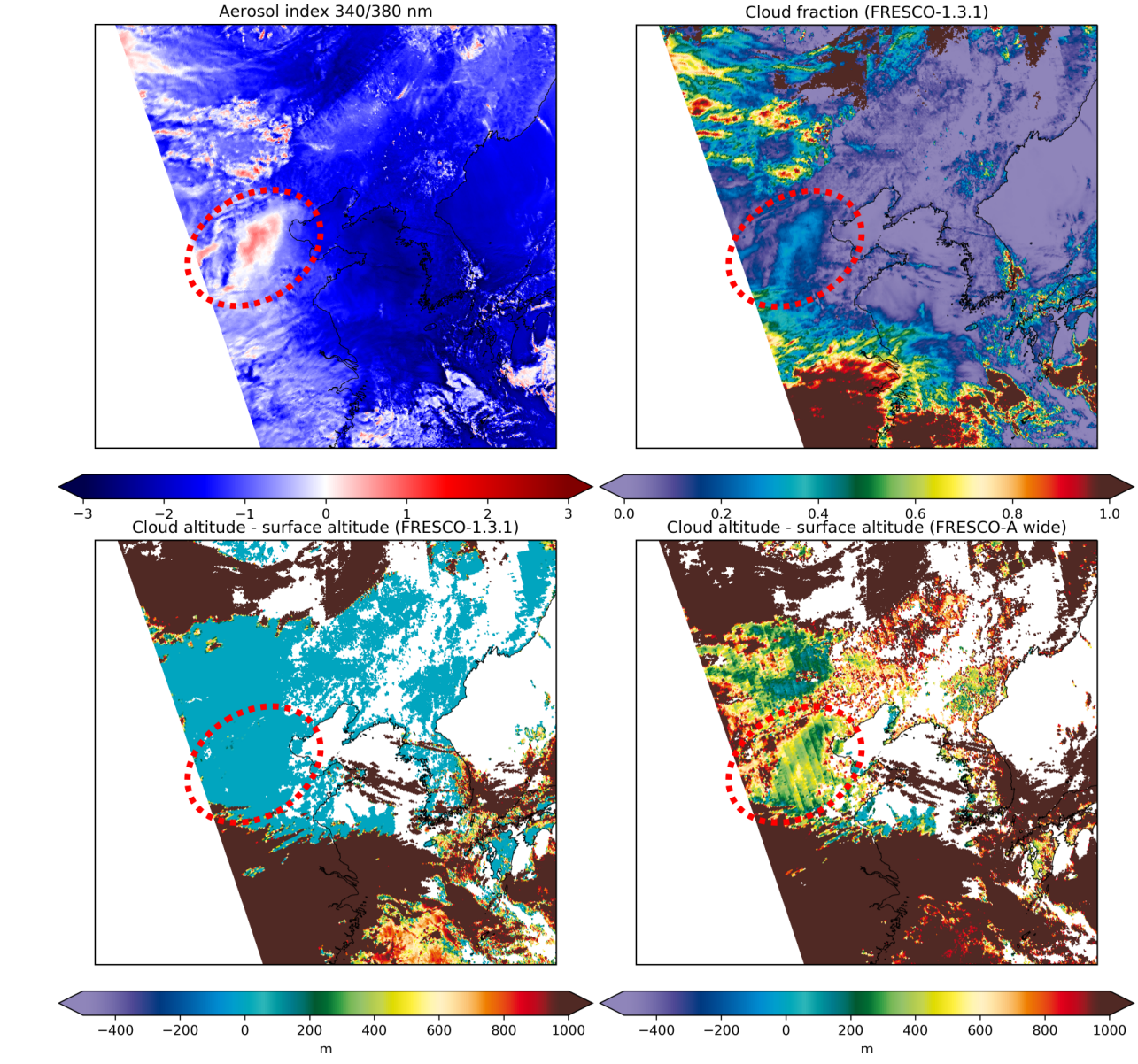

Figure 4. S5P Aerosol Index OFFL 1.2.2 (top left), S5P FRESCO OFFL 1.3.1 cloud fraction (top right), S5P FRESCO OFFL 1.3.1 cloud height offset from the surface (bottom left) and S5P FRESCO wide (version 1.4, product to be released) cloud height offset from the surface (bottom right). Orbit 7062 at 2019-02-23, 1200x1200 km^2 square centered at 38°N, 120°E. The cloud height products are filtered using qa_value > 0.5 and CF > 0.05. The region of interest is indicated by the red-dashed ellipse.

https://doi.org/10.5194/amt-2020-122
Preprint. Discussion started: 29 June 2020

Atmospheric Measurement Techniques Discussions

4.2 Comparison of zonal means between cloud products

In this section zonal mean comparisons are presented for the different cloud products. Fig. 5 presents comparisons at one day (2018-04-28) between S5P OCRA/ROCINN_CAL and VIIRS of RCF and GCF (left panel), CTH (middle panel) and COT (right panel).

S5P OCRA/ROCINN_CAL RCF and VIIRS GCF show a similar latitudinal variation, but, as expected, the geometrical cloud fraction is higher than the S5P OCRA radiometric cloud fraction (Loyola et al., 2010). While the CTH variation is similar, variations are stronger for VIIRS. Finally, COT latitudinal variations are similar for S5P OCRA/ROCINN_CAL and VIIRS, but with an offset (S5P OCRA/ROCINN_CAL higher than VIIRS). Further detail about the comparison between S5P OCRA/ROCINN_CAL and VIIRS is provided in section 4.3.

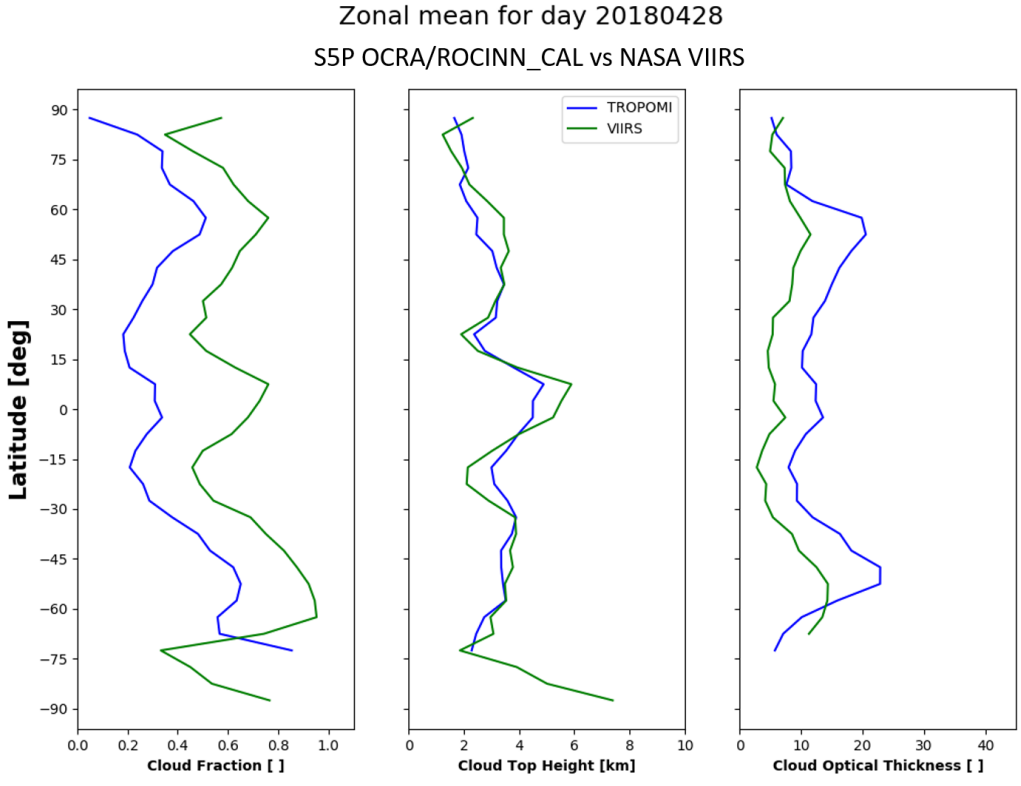

Figure 5. Zonal means for S5P OCRA/ROCINN_CAL (blue) and NASA VIIRS (green). The comparison refers to data from 28th April 2018 (VIIRS cloud fraction is a geometrical cloud fraction whereas the S5P OCRA cloud fraction is a radiometric one).

Fig. 6, left panel, presents a comparison of the zonal means of sRCF of S5P OCRA/ROCINN_CRB, S5P FRESCO and OMCLDO2, and of GCF of MODIS, in function of latitude, at day 2020-02-29. Similar results have been obtained at other days (see Fig. S4). There is a good correspondence between the three products between approximately -60° and +40° latitude.

https://doi.org/10.5194/amt-2020-122
Preprint. Discussion started: 29 June 2020

Atmospheric Measurement Techniques Discussions

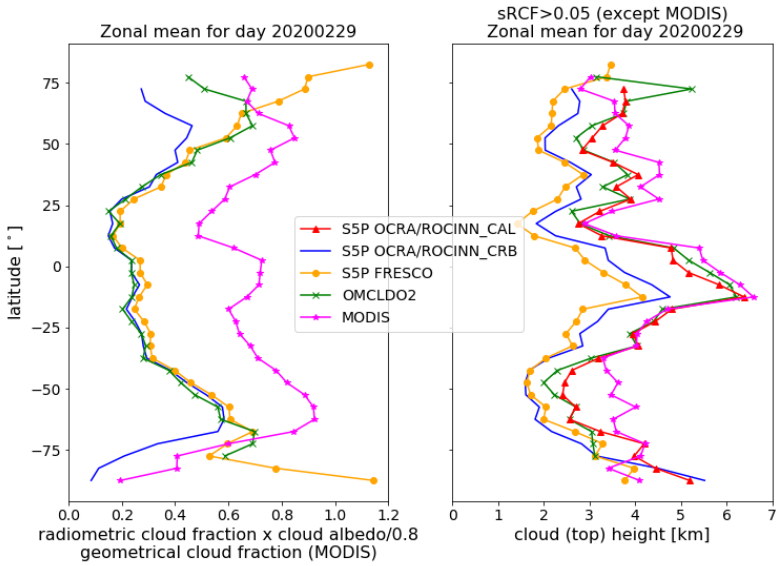

Figure 6. Zonal means at 2020-02-29. Left: scaled radiometric cloud fraction $f_{rc,0.8}$ of S5P OCRA/ROCINN_CRB, S5P FRESCO and OMCLDO2, and geometric cloud fraction of MODIS. Right: cloud height of the same data products, and in addition cloud top height of S5P OCRA/ROCINN_CAL. Here, pixels with $f_{rc,0.8} < 0.05$ are excluded (not applicable to MODIS), as the cloud height becomes highly uncertain at very low cloud fraction. Note that S5P OCRA/ROCINN automatically assigns a fill value to the cloud height when RCF<0.05.

OMCLDO2 and S5P OCRA/ROCINN_CRB have a mean difference in $f_{rc,0.8}$ of 0.005 in this region, while S5P FRESCO $f_{rc,0.8}$ is ~0.03 higher than S5P OCRA/ROCINN_CRB $f_{rc,0.8}$. Beyond this latitude range, the sRCF diverge, with $f_{rc,0.8}$ becoming larger for OMCLDO2 and especially for S5P FRESCO, where the sRCF reaches values up to 1.2. This can likely be attributed to the different treatment of snow-ice cases by the different cloud products. Also indicated on the same figure panel is the GCF of MODIS. The latitudinal variation show roughly similar variations as that of the S5P OCRA/ROCINN_CRB, S5P FRESCO and OMCLDO2, but, again as expected, the geometrical cloud fraction is larger than the scaled radiometric fractions of the other cloud products. Note that at the extreme latitudes, the latitudinal variation of MODIS GCF is rather comparable to that of S5P OCRA/ROCINN than to that of S5P FRESCO.

Fig. 6, right panel, presents a comparison of the zonal means of cloud height of S5P ROCINN_CRB, S5P FRESCO and OMCLDO2, and of the cloud top height of S5P ROCINN_CAL and MODIS. Pixels with $f_{rc,0.8} < 0.05$ are removed (except for MODIS, where RCF is not applicable), as the cloud height uncertainty becomes very high at these low cloud fractions. Note that for S5P ROCINN_CRB and S5P ROCINN_CAL, pixels with RCF < 0.05 are automatically assigned a fill value. While the latitudinal variation of cloud (top) height of the different cloud products are similar, there are also offsets. S5P FRESCO CH is on average a few hunderd meter below S5P OCRA/ROCINN_CRB CH, while S5P OCRA/ROCINN_CAL CTH and OMCLDO2 CH are ~1 km above S5P OCRA/ROCINN_CRB CH.

https://doi.org/10.5194/amt-2020-122
Preprint. Discussion started: 29 June 2020


Atmospheric Measurement Techniques Discussions

MODIS CTH is mostly higher than S5P OCRA/ROCINN_CAL CTH, being about 0.5 to 1 km higher between latitudes $[-60°, -40°]$ and $[+30°, -50°]$. Similar conclusions can be drawn for other days (Fig. S4). The consistently higher MODIS CTH compared to S5P OCRA/ROCINN_CAL CTH is also observed when comparing 1 month of data (Fig. S5). These results are consistent with Schuessler et al. (2014) showing that the ROCINN_CAL model retrieves higher clouds than the ROCINN_CRB model, and also consistent with the results from Loyola et al. (2010) showing higher clouds from infrared sounders compared to ROCINN.

4.3 Comparison between S5P OCRA/ROCINN_CAL and NPP VIIRS

4.3.1 Data selection and processing

For the current study, six days of NASA VIIRS data have been provided to DLR for the initial validation of TROPOMI OCRA/ROCINN_CAL product Version 1. As it was stated earlier, the original NASA VIIRS pixels have a resolution of 750 m and a pixel-by-pixel comparison is only possible if the cloud quantities from both instruments are brought to the same grid. The re-gridding of the original NASA data brought them to the TROPOMI footprints as it is explained by the S5P-NPP Cloud Processor ATBD (Siddans, 2016). The datasets have been filtered according to several criteria to ensure that the comparison is meaningful. Only data with a OCRA/ROCINN_CAL qa_value (this is the quality indicator for the TROPOMI cloud product) above 0.5 were selected. The S5P CLOUD snow/ice flag was used to exclude data over such high reflective surfaces because the cloud retrievals are particularly challenging in these conditions. Furthermore, only pixels with a VIIRS geometrical cloud fraction, which originates from a cloud mask, above 0.9 contributed to the comparison. This filtering was considered necessary in order to mitigate artefacts of the re-gridding process especially at the cloud boundaries and at scattered small-scale clouds. Finally, only pixels which obey to the threshold criteria of CTH<15 km and 1<COT<150 were used for the validation exercise. Those thresholds have been set because the S5P OCRA/ROCINN algorithm in CLOUD version 1 can retrieve clouds up to a maximum CTH of 15 km and with an optical thickness not lower than 1 while the re-gridded VIIRS COT has a maximum of 150. After the aforementioned filtering and harmonization process of the two datasets, the total number of valid pixels for comparison exceeded the number of 30.000.000.

The COT from VIIRS is not comparable directly to the S5P COT because VIIRS has a geometric cloud fraction and not a radiometric one. For this reason we have introduced an effective COT which is the product of COT with the RCF. For the optically thin clouds, the radiometric cloud fraction is underestimated and this results to an overestimated COT. By taking the product COT x RCF, any overestimation of the COT is compensated by the corresponding underestimation of the RCF.

The NASA VIIRS COT is retrieved simultaneously with the effective particle size from the reflection function at 0.75 μm and 2.16 μm. The reflection function at 0.75 μm is in principle sensitive to the COT and the reflection function at 2.16 μm is sensitive to the effective radius (Nakajima and King, 1990). S5P OCRA/ROCINN_CAL COT is retrieved at the continuum of the Oxygen A-band (outside the absorption band). Therefore, the wavelength coverage should have no significant impact on the COT.

https://doi.org/10.5194/amt-2020-122
Preprint. Discussion started: 29 June 2020

Atmospheric Measurement Techniques Discussions

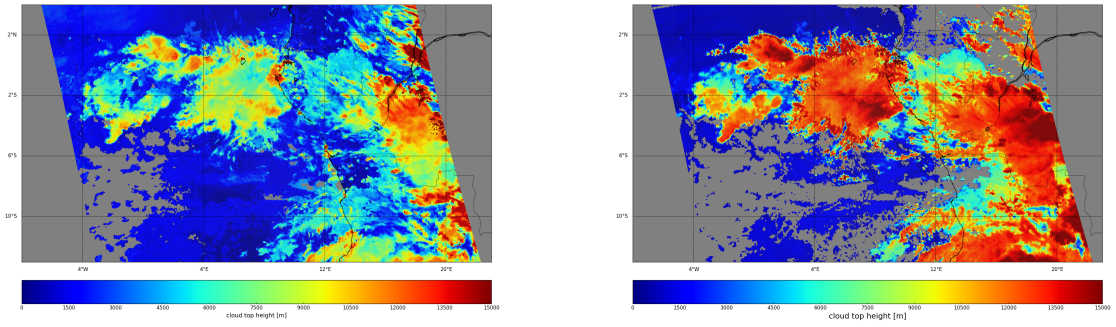

Figure 7. Cloud top height of S5P OCRA/ROCINN_CAL (left) and of regridded NPP VIIRS (right), for orbit 01080.

4.3.2 Results

Fig. 7 presents, for part of orbit 01080, the cloud top height of S5P OCRA/ROCINN_CAL and of NPP VIIRS, after regridding to the same pixel size as S5P CLOUD. Fig. S6 shows the same for cloud optical thickness. While similar cloud features can be discerned in the S5P OCRA/ROCINN_CAL and the NPP VIIRS plots, there are also quantitative differences.

The daily distribution and statistical characteristics do not seem to vary significantly for the several days, as it can be seen from the box plots of Fig. S7. In particular, as far as the COT is concerned, the distribution for TROPOMI is much wider than the one of VIIRS (with a standard deviation of TROPOMI being 22.8 compared to 12.7 for VIIRS) and the median for TROPOMI is about 12 while for VIIRS it is about 7. The first quartile Q1 for both instruments is 3, but the third quartile Q3 is higher in TROPOMI than in VIIRS (i.e., 24 and 15, respectively). For the CTH, the distribution for TROPOMI is narrower than the one for VIIRS with a standard deviation of 2.9 km and 4.0 km for TROPOMI and VIIRS, respectively. The median for TROPOMI is 2.5 km and for VIIRS it is 4 km. Similarly to the COT, the first quartile Q1 is for both sensors the same around 1.8 km. However, the third quartile is for TROPOMI at 6 km and for VIIRS at 9 km.

The general features of the statistical measures can be drawn from Fig. 8, which depict the histograms of the CTH and COT, respectively. The complete dataset including both surface types (land and ocean/water) for the 6 days is used. First of all, one can see that both instruments capture the same CTH mode at around 1.8 km. This mode is mainly dominant over the ocean (see Figure S8 in the supplementary information) and it refers to the low-level marine stratocumulus clouds. Differences at the tails for the CTH distributions are present. TROPOMI seems to underestimate the high level clouds with CTH larger than 8 km. The mean TROPOMI CTH is lower than the one from VIIRS (3.8 km and 5.4 km, respectively). The observed negative bias is in the order of 1.6 km. As will be seen in Section 4.4, a negative bias is also observed from the Cloudnet comparison. Therefore this is a general outcome of the CTH validation using independent sensors. Regarding the COT, TROPOMI seems to overestimate this cloud parameter meaning that the clouds appear optically thicker than in VIIRS. The S5P ROCINN overestimation is

https://doi.org/10.5194/amt-2020-122
Preprint. Discussion started: 29 June 2020

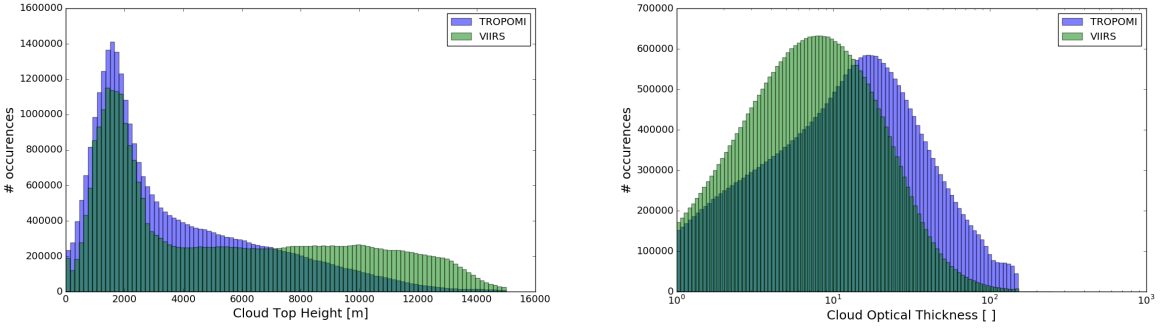

Figure 8. Histograms of the CTH (top) and COT (bottom) for TROPOMI and VIIRS. The complete dataset is considered.

consistent with the GOME ROCINN results from (Loyola et al., 2010). The mean COT from VIIRS was found at 11.4 whereas the mean COT of TROPOMI is found at 19.2 leading to a positive bias of 7.9. The positive bias in the COT and the negative bias in the CTH has been also initially seen from the zonal means (see Figure 9 and Figure 10). The explanation for those biases are mainly related to the fact that S5P OCRA/ROCINN_CAL assumes liquid-water clouds and their properties stem from the Mie scattering theory. The ice clouds are not parameterized with the current S5P ROCINN_CAL algorithm in CLOUD version 1 but they will be included in future versions. While water clouds are assumed to be composed entirely by spherical droplets, ice clouds consist of a variety of habits (i.e., mixtures of randomly-oriented hexagonal plates and columns, two dimensional bullet rosettes and aggregated). The direct impact of the cloud microphysics to the retrieved COT is discussed in Zeng et al. (2012).

The similarities of the two datasets can be well summarized through the Taylor diagram (Taylor, 2001) which is shown in Figure S9. The correlation coefficients for the cloud parameters CTH and COT are shown based on the surface type. The CTH is highly correlated for both surface types with the correlation coefficient r being 0.86 and 0.74 over water and land, respectively. Similarly, the COT appears with a higher correlation coefficient r=0.66 over water in comparison to 0.48 over land. The low correlation coefficients for the COT over land might be due to non-realistic surface albedo values (extracted from a climatology). Usually, over land the surface albedo might change more rapidly than over water. From the Taylor diagram much more information can be extracted. The CTHs for land and water, which are lying in the inner area of the dashed arc, imply that the corresponding dataset has a lower standard deviation and indicates that the pattern variations are of a decreased amplitude. The COTs for land and water, which are lying in the outer area, imply that the pattern variations are higher than expected. Moreover, the CTH appears with lower Root-Mean-Square (RMS) errors than the COT.

The agreement between NASA VIIRS and S5P OCRA/ROCINN_CAL seems to be much better for the low-level clouds which usually consist of liquid water particles. The main question is how well the two sensors agree for the several cloud types. For identifying in which type of clouds the differences are larger we follow the ISCCP (International Satellite Cloud Climatology Project) classification (Schiffer and Rossow, 1983). The scheme depicted in Fig. S10 classifies the clouds based on their CTH and COT combinations. Cumulus, stratocumulus and stratus are the low-level clouds, the altocumulus, altostratus

https://doi.org/10.5194/amt-2020-122
Preprint. Discussion started: 29 June 2020


Atmospheric Measurement Techniques Discussions

and nimbostratus are the mid-level clouds and finally, the cirrus, cirrostratus and deep convective are classified as high-level clouds. The biases for all low-, mid- and high-level clouds are summarized in Table S1. Cumulus and stratocumulus (low-level clouds) over water appear 50% of the time with small negative CTH biases of a few hundred meters. The largest COT bias among the low-level clouds appears for the stratus type over water, but these type of clouds are not so frequent. From the mid-level clouds (see Table S1) the altocumuli show a low CTH bias, but the other two types (among which the most frequent is the altostratus), have a negative bias of about 1.5 km. Altostratus and nimbostratus over water appear with a high positive bias in the COT. Finally, from the high-level clouds, the cirrostratus and cirrus, which appear with a frequency higher than 80%, show high biases in both CTH and COT. All in all, the agreement between VIIRS and TROPOMI cloud properties is certainly best for low level clouds and worse for high-level clouds.

4.4 Comparison of S5P cloud height with CLOUDNET

In this section we discuss the comparison of S5P OCRA/ROCINN_CAL CTH, S5P OCRA/ROCINN_CRB CH and S5P FRESCO CH with ground-based CLOUDNET data. Moreover, we compare also OMI OMCLDO2 with CLOUDNET, using the same methodology. Aura/OMI has a similar overpass time as S5P/TROPOMI. Like S5P CLOUD and FRESCO, OMCLDO2 provides rather effective cloud heights which are used as input in the retrieval of atmospheric gases. By comparing the S5P products with the CLOUDNET data on one hand, and OMCLDO2 with CLOUDNET data on the other hand, one learns better how the effective cloud heights of these different products relate to the (vertically resolved) lidar/radar cloud observations of CLOUDNET, and where they are different. It also allows to make the connection with the work of Veefkind et al. (2016). It should be noted that other OMI cloud products could have been taken here for comparison, like the OMCLDRR which is based on the Fraunhofer filling signatures (346-354 nm) to derive effective cloud fraction and cloud optical centroid pressure (Joiner and Vasilkov, 2006), but this is beyond the scope of the current work.

In this comparison, we have used S5P CLOUD RPRO and OFFL files with processor version 1.1.7, and S5P FRESCO RPRO+OFFL files with processor version 1.3, from 2018-04-30, to 2020-02-27.

Satellite - CLOUDNET comparison pairs are established as follows.

- Where applicable, the satellite RCF is converted to an sRCF, at CA=0.8.
- Satellite pixels are selected only if they cover the CLOUDNET site, have a qa value>50% (S5P) or no error flag (OMCLDO2), and have sRCF > 0.05.
- All CLOUDNET measurements within ± 600 s of a S5P or OMCLDO2 overpass are considered. From these, the CLOUDNET cloud occurrence fraction (COF), mean CLOUDNET CTH h_{ct} and CMH h_{cm}, and standard deviation of CLOUDNET CTH $\sigma(h_{ct})$ and CMH $\sigma(h_{cm})$ are calculated.
- To limit temporal variability, co-locations are selected only if CLOUDNET COF < 50%, $\sigma(h_{ct}) < 0.5$ km and $\sigma(h_{cm}) < 0.5$ km.

https://doi.org/10.5194/amt-2020-122
Preprint. Discussion started: 29 June 2020


Atmospheric Measurement Techniques Discussions

Despite these filter criteria, some comparison error due to co-location mismatch will persist. Another, more fundamental, problem is that the cloud (top) heights obtained from the radar-lidar based CLOUDNET data on one hand, and the more 'effective' cloud (top) heights of the S5P and OMI products are not fully comparable. For example, while the CLOUDNET CMH is obtained as a simple mean of all 'cloudy' grid positions (regardless of the local optical thickness), the cloud (top) heights returned by the S5P and OMI cloud products do depend on optical thickness. Moreover, none of the S5P or OMI cloud products take into account the possibility that a cloud can be multi-layered.

Fig. 9 presents comparisons between satellite (OMCLDO2 CH, S5P OCRA/ROCINN_CAL CTH, S5P OCRA/ROCINN_CRB CH, S5P FRESCO CH) and CLOUDNET, at the site Juelich. Co-location pairs are ordered along CLOUDNET CTH. Similar plots are provided in the supplement for the other sites.

Furthermore, normed histograms and associated estimated probability density distributions of OMCLDO2 CH vs CLOUDNET CTH, and S5P OCRA/ROCINN_CAL CTH vs CLOUDNET CTH, are provided in Fig. 10. Similar plots are provided in the supplement, Section S4 for the other sites, with the exclusion of sites with less than 70 co-located data pairs, and of the site Summit, where most satellite cloud height retrievals are problematic.

Following conclusions can be drawn:

- Co-location pairs with a low satellite RCF are more scattered, in line with the higher cloud height uncertainty.

- **OMCLDO2 vs CLOUDNET.** There are far fewer co-locations with CLOUDNET available for OMCLDO2 than for the S5P cloud products, showing a clear advantage for S5P. For the lowest (CLOUDNET CTH$\lessapprox$2 km; mostly liquid) clouds, OMCLDO2 CH corresponds to the CLOUDNET CTH. At CLOUDNET CTH $\gtrapprox$3 km, OMCLDO2 CH rather corresponds to the CLOUDNET CMH (e.g., Juelich, Palaiseau, Mace Head) or is below the CLOUDNET CMH (e.g., Munich, Schneefernerhaus, Leipzig). The latter pattern was also seen at Cabauw by Veefkind et al. (2016) (their figure 10). At Juelich, both CLOUDNET CTH and OMCLDO2 CH distributions (Fig. 10) have a low-altitude local mode at a well-matching ≈2 km. Also, for several other sites, the low-altitude mode agrees within 20% (Fig. 11), but there are also exceptions (Lindenberg, Norunda, Ny Alesund).

- **S5P OCRA/ROCINN_CAL vs CLOUDNET.** On average, CLOUDNET CTH $\gtrapprox$ S5P OCRA/ROCINN_CAL CTH $\gtrapprox$ CLOUDNET CMH. For the higher clouds (CLOUDNET CTH$\gtrapprox$4 km) it is in most cases closer to CLOUDNET CMH. The low-altitude local CTH modes of CLOUDNET and S5P OCRA/ROCINN_CAL are reasonably well matched: in most cases they agree within 20% (Fig. 11). At several sites (e.g., Graciosa island, Juelich, Chilbolton) a higher altitude CTH mode is also captured by S5P OCRA/ROCINN_CAL, but shifted towards lower altitude compared to CLOUDNET CTH. Mean and median S5P OCRA/ROCINN_CAL CTH are lower than those of CLOUDNET, mainly due to the CTH mismatch of the higher altitude clouds which have an ice component.

- **S5P OCRA/ROCINN_CRB and S5P FRESCO vs CLOUDNET.** S5P OCRA/ROCINN_CRB CH and S5P FRESCO CH are on average below CLOUDNET CMH for clouds with CLOUDNET CTH$\lessapprox$4 km. For higher clouds the satellite CH rather corresponds to CLOUDNET CMH. It can be seen from Fig. 9 that in a number of cases S5P FRESCO and

https://doi.org/10.5194/amt-2020-122
Preprint. Discussion started: 29 June 2020

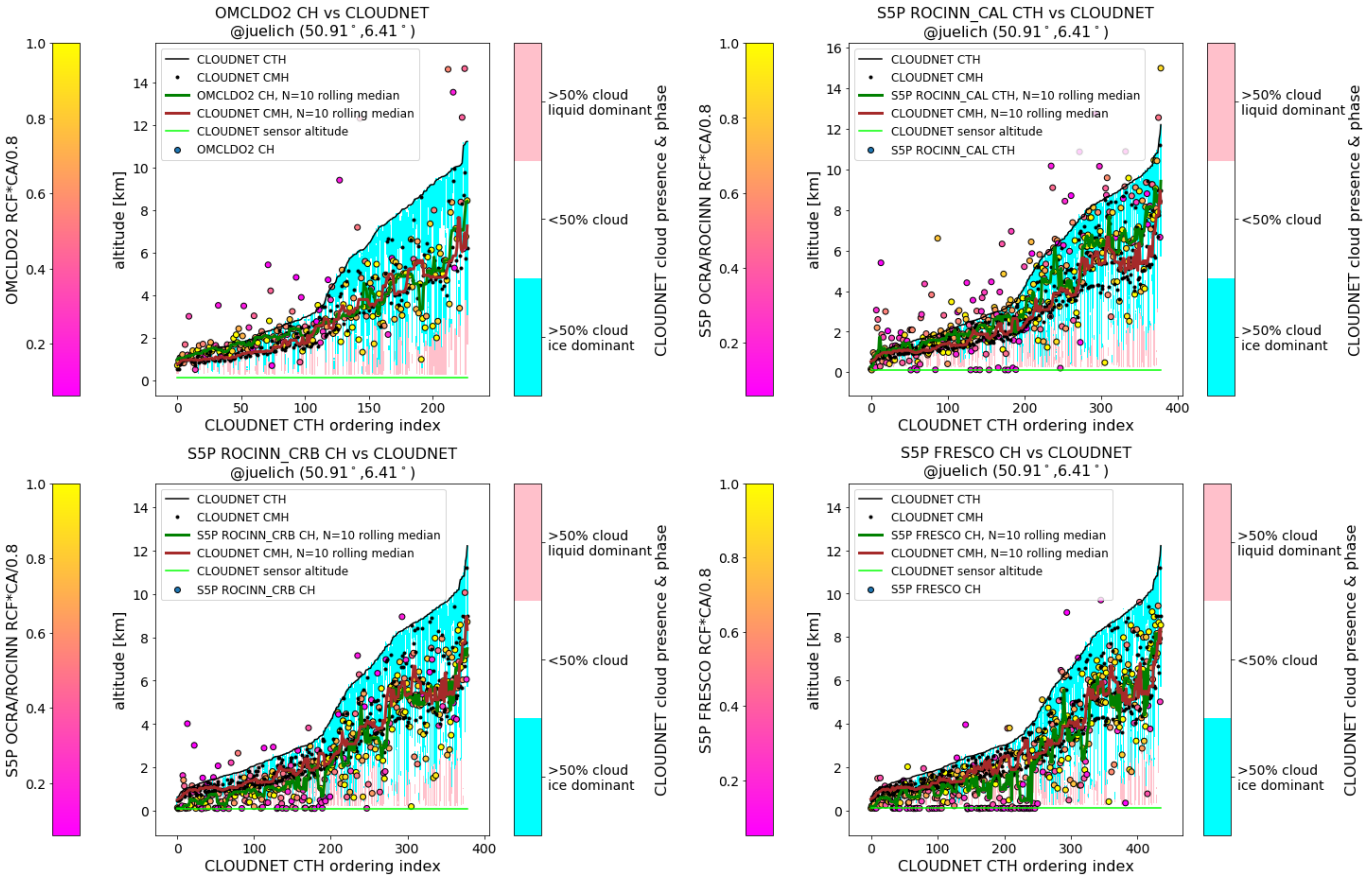

Figure 9. Comparisons of OMCLDO2 CH (top left), S5P OCRA/ROCINN_CAL CTH (top right), S5P OCRA/ROCINN_CRB CH (bottom left) and S5P FRESCO CH (bottom right) with CLOUDNET, at the site Juelich. Co-location pairs are ordered along CLOUDNET CTH. Black line indicates the CLOUDNET CMH. Satellite data points are coloured based on the sRCF. A 20-point window rolling median (green line) based on the satellite data is added as well. A heat map is added based on the CLOUDNET vertical classification, to distinguish regions with no cloud or small cloud presence (white), liquid cloud presence (red) and ice cloud presence (blue).

https://doi.org/10.5194/amt-2020-122
Preprint. Discussion started: 29 June 2020

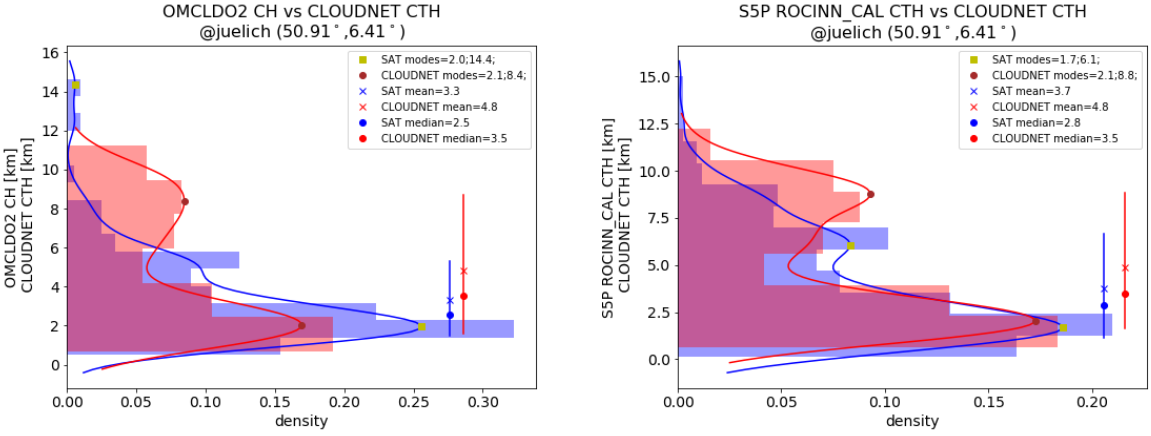

Figure 10. Normed histograms of satellite-CLOUDNET co-located cloud height or cloud top height, with superimposed density estimates using Gaussian kernels (from the python scipy.stats package), at the site Juelich. OMCLDO2 CH vs CLOUDNET CTH (left) and S5P OCRA/ROCINN_CAL CTH vs CLOUDNET CTH (right). The most important local modes of the satellite and CLOUDNET distributions are indicated, as well as mean, median and the central 68% interval.

S5P OCRA/ROCINN_CRB retrieve a cloud height equal to the surface altitude. This contributes at least partly to the on average lower S5P OCRA/ROCINN_CRB CH and S5P FRESCO CH compared to CLOUDNET CMH. Ground height retrievals occur also for S5P OCRA/ROCINN_CAL, but to a far less extent. It does not occur for OMCLDO2.

Local conditions can impact the comparison:

- The CLOUDNET station at Schneefernerhaus is located at a mountain, at 2.7 km, while the surface altitude attributed to the relatively coarse satellite pixels is generally lower. This causes a mismatch in cloud height for low altitude clouds, where the cloud height observed by the satellite can be below the station altitude.

- Ny-Alesund can be affected by snow-ice conditions and as a consequence a high surface albedo, which is a challenge for satellite cloud retrievals. Different satellite products can be affected in different ways. OMCLDO2 is characterized by many zero-offset cloud heights with a high sRCF. For S5P OCRA/ROCINN_CAL, S5P OCRA/ROCINN_CRB and S5P FRESCO, one notices a significant number of low-sRCF data points where the retrieved cloud height is significantly overestimating the CLOUDNET CTH.

- Summit is covered by permanent ice. OMCLDO2 overestimates the CLOUDNET CTH. For most data points of S5P OCRA/ROCINN_CAL, S5P OCRA/ROCINN_CRB and S5P FRESCO, zero offset clouds are obtained.

Figs. 12 and 13 present boxplot comparisons between the S5P cloud products cloud (top) height and CLOUDNET height, with indications of the mission requirements on bias and uncertainty; the latter is compared here with a robust dispersion estimator: 0.5 of the central 68 interpercentile interval (0.5 IP68), which amounts to one standard deviation in the ideal case

https://doi.org/10.5194/amt-2020-122
Preprint. Discussion started: 29 June 2020

Atmospheric Measurement Techniques Discussions

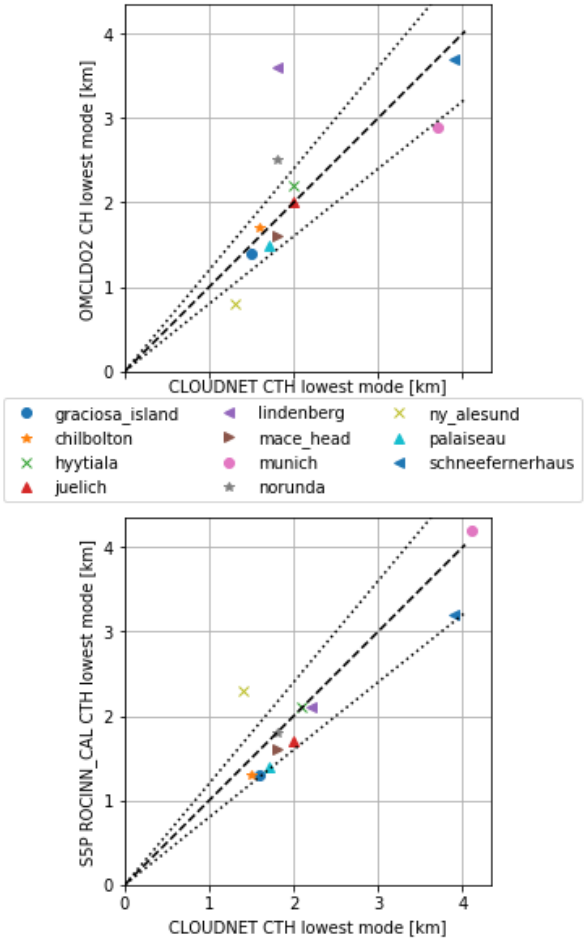

Figure 11. Top. Correlation plot between the lowest CTH modes of OMCLDO2 and CLOUDNET. Only sites with more than 70 co-location pairs are considered. Dashed line is the 1:1 line, dashed lines are the $\pm 20\%$ deviations from the 1:1 line. Bottom. The same, but between the lowest CTH modes of S5P OCRA/ROCINN_CAL and CLOUDNET.

https://doi.org/10.5194/amt-2020-122
Preprint. Discussion started: 29 June 2020


Atmospheric Measurement Techniques Discussions

of a Gaussian error distribution. It should be noted that apart from satellite error, several other components contribute to the bias and dispersion: measurement error in the ground-based data, temporal and spatial co-location mismatch, and the fact that the effective cloud heights from satellite, and those from CLOUDNET, are not fully comparable. In particular regarding the calculated dispersion vs the stated uncertainty requirement, it must be clear that this can only serve as a partial quality test. If the dispersion is *lower* than the uncertainty threshold, one can be confident that the satellite uncertainty is within the threshold. If, on the other hand, the dispersion is *higher* than the uncertainty threshold, it is by no means a proof that the satellite data exceeds the uncertainty threshold.

Fig. 12 presents boxplot comparisons between S5P OCRA/ROCINN_CAL CTH and CLOUDNET CTH, and between S5P OCRA/ROCINN_CAL CTH and CLOUDNET CMH. In agreement with the above results, S5P OCRA/ROCINN_CAL CTH minus CLOUDNET CTH is characterized by a negative bias, bordering to or exceeding the 20% bias requirement. However, if one compares S5P OCRA/ROCINN_CAL CTH with the CLOUDNET CMH, the bias requirement is fulfilled in most cases. Dispersions are calculated here using a robust estimator: 0.5 of the central 68 interpercentile interval (0.5 IP68) which amounts to one standard deviation in the ideal case of a Gaussian error distribution. The dispersion exceeds the 0.5 km uncertainty threshold in almost all cases (but see the note on the calculated bias and dispersion vs. bias and uncertainty thresholds above).

Fig. 13 presents boxplot comparisons between S5P OCRA/ROCINN_CRB CH and CLOUDNET CMH, and between S5P FRESCO CH and CLOUDNET CMH. A negative bias is observed at almost all sites, often exceeding the 20% bias requirement. Again, the dispersion exceeds the 0.5 km uncertainty threshold in almost all cases (but see the note on the calculated bias and dispersion vs. bias and uncertainty thresholds above).

5 Discussion and conclusions

The TROPOMI cloud products S5P OCRA/ROCINN_CAL, S5P OCRA/ROCINN_CRB and S5P FRESCO are validated in this work, using independent satellite data (NPP VIIRS, MODIS and OMI OMCLDO2) and ground-based CLOUDNET data. The following conclusions are obtained.

- S5P OCRA/ROCINN RCF and C(T)H can exhibit enhanced values at the east swath edge and a N-S gradient in the cloud albedo. This is expected to improve with the to-be-released S5P CLOUD version 2.
- S5P FRESCO has a tendency to retrieve at low cloud fraction a cloud height equal to the surface altitude. This is expected to improve with the to-be-released S5P FRESCO 1.4 version.
- In the comparison of zonal means between different satellite products, similar latitudinal variations in cloud fraction, cloud (top) height and cloud optical thickness are obtained, sometimes with offsets. Radiometric cloud fractions, scaled to a fixed cloud albedo, between S5P OCRA/ROCINN, S5P FRESCO and OMCLDO2 agree well, except at extreme latitude where S5P FRESCO diverges.
- CTH and COT of S5P OCRA/ROCINN_CAL and NPP VIIRS CTH agree best for low-level liquid clouds, while they disagree for the high-level clouds. A similar conclusion is reached when comparing S5P OCRA/ROCINN_CAL CTH

https://doi.org/10.5194/amt-2020-122
Preprint. Discussion started: 29 June 2020

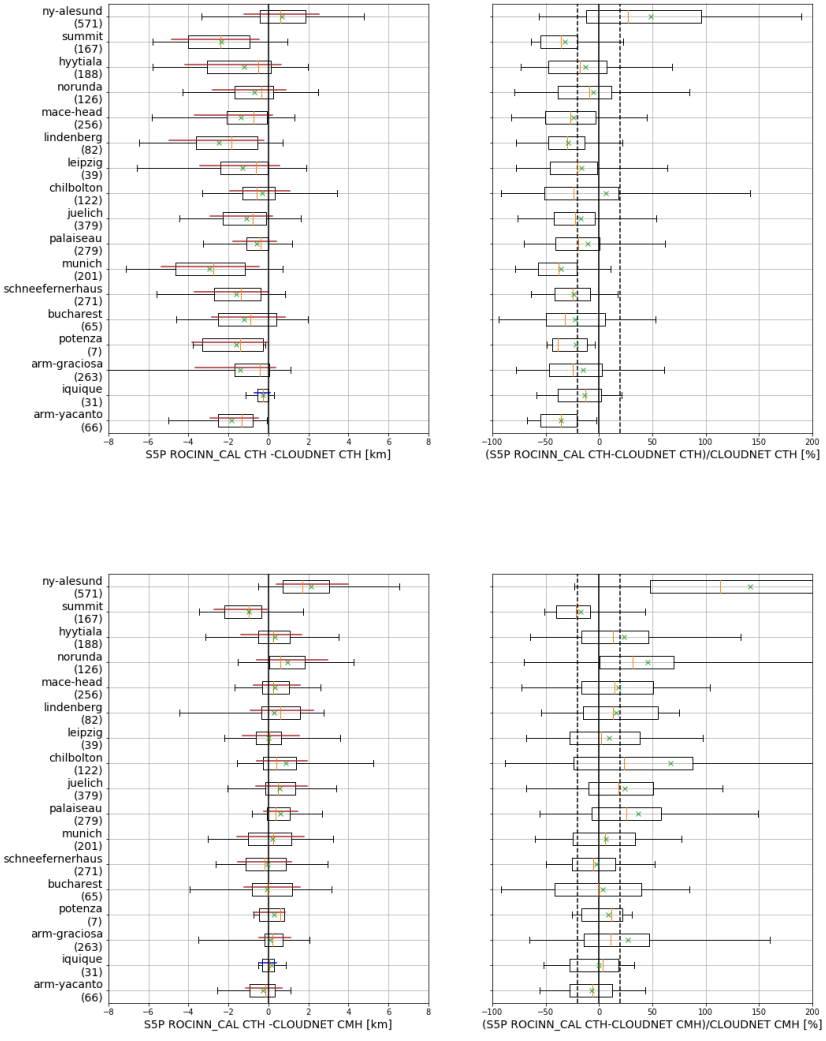

Figure 12. Top. Boxplot of the difference (left), and relative difference (right) between S5P OCRA/ROCINN_CAL CTH and CLOUDNET CTH. Bottom. The same but between S5P OCRA/ROCINN_CAL CTH and CLOUDNET CMH. Figure conventions are as follows. Box edges: first and third quartile; line: median; whiskers: 5 and 95 percentiles; cross: median. Furthermore, a line corresponding to the central 68% interval is indicated. Its color is brown when the 0.5 IP68 exceeds the dispersion requirement, and green otherwise.

https://doi.org/10.5194/amt-2020-122
Preprint. Discussion started: 29 June 2020

Atmospheric Measurement Techniques Discussions

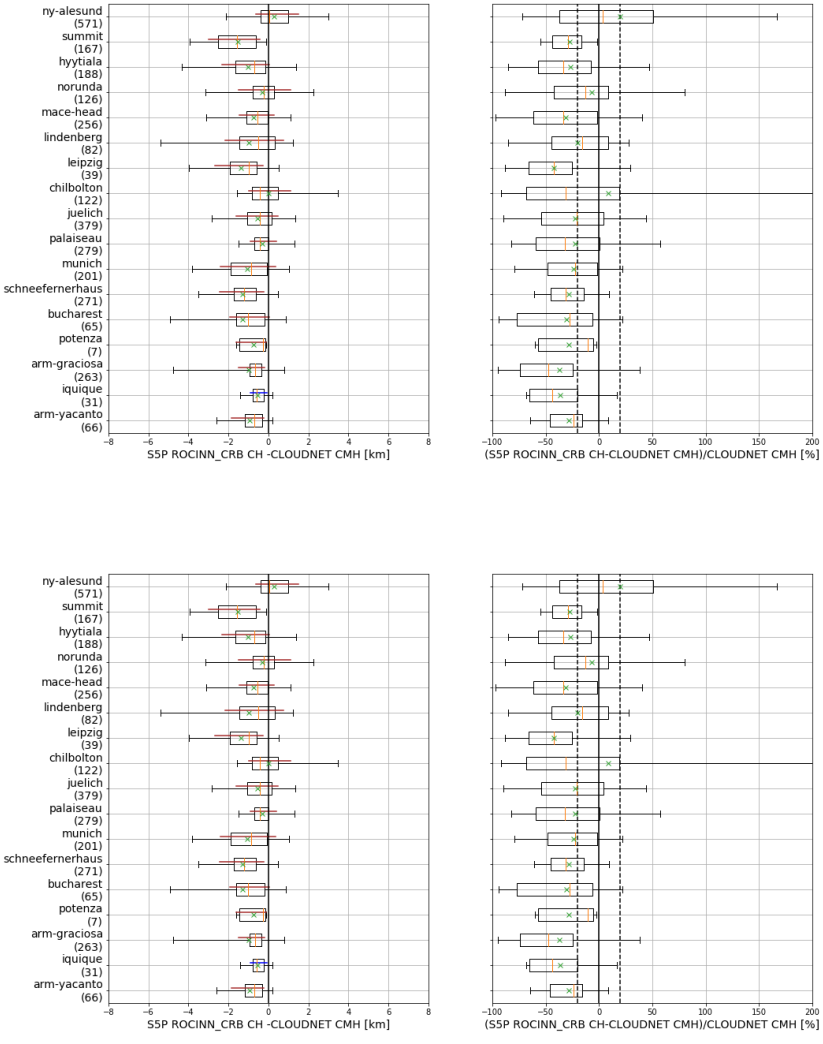

Figure 13. Top. Boxplot of the difference (left), and relative difference (right) between S5P OCRA/ROCINN_CRB CH and CLOUDNET CMH. Bottom. The same but between S5P FRESCO CH and CLOUDNET CMH. The same conventions as in Fig. 12 are followed.

https://doi.org/10.5194/amt-2020-122
Preprint. Discussion started: 29 June 2020


Atmospheric Measurement Techniques Discussions

with ground-based CLOUDNET CTH. In a future release of S5P CLOUD, liquid clouds and ice clouds will be retrieved separately. Then an improved agreement with NPP VIIRS and CLOUDNET can be expected.

- The different S5P cloud products, and OMCLDO2, track different vertical portions of a cloud (as observed by CLOUDNET). For low clouds, OMCLDO2 CH corresponds to the CLOUDNET CTH, while S5P OCRA/ROCINN_CRB CH and S5P FRESCO CH are below the CLOUDNET CMH. For higher clouds, OMCLDO2 CH is sometimes at, but also sometimes below, the CLOUDNET CMH. This is in line with expectations: there is a reduced sensitivity for high clouds due to the reduced absorption at low pressures due to the density-squared nature of the absorption feature. On the other hand, S5P OCRA/ROCINN_CRB CH and S5P FRESCO CH rather follow the CLOUDNET CMH for high clouds. S5P OCRA/ROCINN_CAL CTH is mostly somewhere between the CLOUDNET CMH and the CLOUDNET CTH.
- As opposed to ROCINN_CRB and FRESCO (both based on a Lambertian model), ROCINN_CAL (based on Mie scattering cloud model), is well able to match the lowest CTH mode of the CLOUDNET observations. At several CLOUDNET sites, ROCINN_CAL also observes a second high mode, but shifted towards smaller CTH compared to the CLOUDNET CTH. Furthermore, S5P OCRA/ROCINN_CAL CTH has far less a tendency to retrieve a cloud height equal to the surface altitude.

Several improvements in the cloud products are foreseen in upcoming version releases. These new data versions should be validated with the same system as used in the current paper, allowing the necessary independent assessment of the S5p data product evolution.

Data availability. Sentinel-5p CLOUD OCRA/ROCINN RPRO (reprocessed) and OFFL (offline) data 1.1.7 can be obtained from the Sentinel-5P Pre-Operations Data Hub (https://s5phub.copernicus.eu/dhus/). Sentinel-5p FRESCO data files are not publicly available, but the FRESCO cloud properties are available in Sentinel-5p NO_2 data files, also at the Sentinel-5P Pre-Operations Data Hub. CLOUDNET data is available from http://cloudnet.fmi.fi/ or from EVDC (ESA Atmospheric Validation Data Centre, https://evdc.esa.int/). Aqua MODIS MYD08_D3 data can be obtained from https://ladsweb.modaps.eosdis.nasa.gov. Aura OMI OMCLDO2 data can be obtained from https://disc.gsfc.nasa.gov/datasets/OMCLDO2_003/summary.

Author contributions. SC and AA carried out the global validation analysis, with support from RL and MS. JCL, DH, AK and TV contributed input and advise at all stages of the analysis. AA, DL, RL and FR developed the OCRA/ROCINN retrieval algorithms and the corresponding operational UPAS processors for TROPOMI, GOME-2 and GOME at DLR. MS, PS and PW developed the TROPOMI and OMI cloud data processors at KNMI. AMF and EOC post-processed Cloudnet data tailored to S5p validation and contributed ground-based scientific expertise. All authors revised and commented on the manuscript.

Competing interests. The authors declare that they have no conflict of interest.

https://doi.org/10.5194/amt-2020-122
Preprint. Discussion started: 29 June 2020

Atmospheric Measurement Techniques Discussions

Acknowledgements. Part of the reported work was carried out in the framework of the Copernicus Sentinel-5 Precursor Mission Performance Centre (S5P MPC), contracted by the European Space Agency (ESA/ESRIN, Contract No.4000117151/16/I-LG) and supported by the Belgian Federal Science Policy Office (BELSPO), the Royal Belgian Institute for Space Aeronomy (BIRA-IASB), the Netherlands Space Office (NSO), and the German Aerospace Centre (DLR). Part of this work was also supported by the S5P Validation Team (S5PVT) AO project CHEOPS-5p (ID #28587, Co-PIs J.-C. Lambert and A. Keppens, BIRA-IASB) with national funding from the BELSPO/ProDEx project TROVA-E2 (PEA 4000116692). The authors express special thanks to B. Langerock, A.M. Fjæraa, J. Granville, S. Niemeijer and O. Rasson for post-processing of the network and satellite data and for their dedication to the S5p operational validation.

This work contains modified Copernicus Sentinel-5 Precursor data (2018-2020) processed by DLR and KNMI, and post-processed by BIRA-IASB. We acknowledge the ACTRIS RI and the ACTRIS-2 project (European Commission contract H2020-INFRAIA, grant no. 654109) for providing the ground-based data from the Cloudnet sites in this study, which was produced by the Finnish Meteorological Institute, and is available for download from http://cloudnet.fmi.fi/. The cloud radar, ceilometer and microwave radiometer data for the ARM sites used in this study (Graciosa and Villa Yacanto) were obtained from the Atmospheric Radiation Measurement (ARM) user facility, managed by the Office of Biological and Environmental Research for the U.S. Department of Energy Office of Science. The cloud radar, ceilometer and microwave radiometer data for the Summit Station were obtained from NOAA; overall programmatic and logistical support for was provided by the US National Science Foundation, with additional instrumental support provided by the NOAA Earth System Research Laboratories, the DOE Atmospheric Radiation Measurement Program, and Environment Canada. We warmly thank the PIs and staff at all stations for their sustained effort in maintaining high quality measurements and for valuable scientific discussions.

We also thank Steven Platnick and co-workers for the provision of prototype 2018 files of NPP-VIIRS to DLR. The Aqua/Modis Aerosol Cloud Water Vapor Ozone Daily L3 Global 1Deg CMG dataset (http://dx.doi.org/10.5067/MODIS/MYD08_D3.061) was acquired from the Level-1 and Atmosphere Archive & Distribution System (LAADS) Distributed Active Archive Center (DAAC), located in the Goddard Space Flight Center in Greenbelt, Maryland (https://ladsweb.nascom.nasa.gov/).

https://doi.org/10.5194/amt-2020-122
Preprint. Discussion started: 29 June 2020

Atmospheric Measurement Techniques Discussions

References

Acarreta, J. R., De Haan, J. F., and Stammes, P.: Cloud pressure retrieval using the O_2 -O_2 absorption band at 477 nm, J. Geophys. Res., 109, D05 204, https://doi.org/10.1029/2003jd003915, 2004.

Anderson, G. P., Clough, S. A., Kneizys, F. X., Chetwynd, J. H., and Shettle, E. P.: AFGL Atmospheric Constituent Profiles, Tech. Rep. AFGL-TR-86-0110, Air Force Geophysics Laboratory, Hanscom AFB, MA, http://www.dtic.mil/cgi-bin/GetTRDoc?AD=ADA175173, 1986.

Bovensmann, H., Burrows, J. P., Buchwitz, M., Frerick, J., Noël, S., Rozanov, V. V., Chance, K. V., and Goede, A. P. H.: SCIAMACHY: Mission Objectives and Measurement Modes, J. Atmos. Sci., 56, 127–150, https://doi.org/10.1175/1520-0469(1999)056<0127:SMOAMM>2.0.CO;2, 1999.

Burrows, J. P., Weber, M., Buchwitz, M., Rozanov, V., Ladstätter-Weißenmayer, A., Richter, A., DeBeek, R., Hoogen, R., Bramstedt, K., Eichmann, K.-U., Eisinger, M., and Perner, D.: The Global Ozone Monitoring Experiment (GOME): Mission Concept and First Scientific Results, J. Atmos. Sci., 56, 151–175, https://doi.org/10.1175/1520-0469(1999)056<0151:TGOMEG>2.0.CO;2, 1999.

ESA: Copernicus Sentinels 4 and 5 Mission Requirements Traceability Document, Tech. Rep. EOP-SM/2413/BV-bv, ESA, https://sentinel.esa.int/documents/247904/2506504/Copernicus-Sentinels-4-and-5-Mission-Requirements-Traceability-Document.pdf, 2017a.

ESA: Sentinel-5 Precursor Calibration and Validation Plan for the Operational Phase, Tech. Rep. ESA-EOPG-CSCOP-PL-0073, ESA, https://sentinel.esa.int/documents/247904/2474724/Sentinel-5P-Calibration-and-Validation-Plan.pdf, 2017b.

Eskes, H. J., van Geffen, J., Boersma, K., Sneep, M., ter Linden, M., Richter, A., Beirle, S., and Veefkind, J. P.: High spatial resolution nitrogen dioxide tropospheric column observations derived from Sentinel-5P TROPOMI observations, Atmos. Meas. Tech. Discuss., pp. preprint, submitted to AMT, April 2020., 2020.

Fishman, J., Watson, C., Larsen, J., and Logan, J.: Determination of Tropospheric Ozone Determined from Satellite Data, J. Geophys. Res. -Atmospheres, 95, 3599–3617, 1990.

Heidinger, A. and Li, Y.: Enterprise AWG cloud height algorithm (ACHA) - Algorithm Theoretical Basis Document. Version 3.3, Tech. rep., NOAA NESDIS Center for Satellite Applications and Research, https://docs.google.com/document/d/1m2SatR91WIJcaAZweongcFCb6Wsx_xnRUcZxp94gXHk/edit, 2019.

Heidinger, A. K., Bearson, N., Foster, M. J., Li, Y., Wanzong, S., Ackerman, S., Holz, R. E., Platnick, S., and Meyer, K.: Using Sounder Data to Improve Cirrus Cloud Height Estimation from Satellite Imagers, J. Atmos. Oceanic Technol., 36, 1331–1342, https://doi.org/10.1175/JTECH-D-18-0079.1, 2019.

Illingworth, A. J., Hogan, R. J., O'Connor, E. J., Bouniol, D., Delanoë, J., Pelon, J., Protat, A., Brooks, M. E., Gaussiat, N., Wilson, D. R., Donovan, D. P., Baltink, H. K., van Zadelhoff, G.-J., Eastment, J. D., Goddard, J. W. F., Wrench, C. L., Haeffelin, M., Krasnov, O. A., Russchenberg, H. W. J., Piriou, J.-M., Vinit, F., Seifert, A., Tompkins, A. M., and Willén, U.: Cloudnet, Bull. Am. Meteorol. Soc., 88, 883–898, https://doi.org/10.1175/bams-88-6-883, 2007.

Ingmann, P., Veihelmann, B., Langen, J., Lamarre, D., Stark, H., and Courrèges-Lacoste, G. B.: Requirements for the GMES Atmosphere Service and ESA's implementation concept: Sentinels-4/-5 and -5p, Remote Sens. Environ., 120, 58 – 69, https://doi.org/https://doi.org/10.1016/j.rse.2012.01.023, the Sentinel Missions - New Opportunities for Science, 2012.

JCGM: Evaluation of measurement data - Guide to the expression of uncertainty in measurement, Tech. rep., Joint Committee for Guides in Metrology (JCGM), http://www.bipm.org/utils/common/documents/jcgm/JCGM_100_2008_E.pdf, 2008.

https://doi.org/10.5194/amt-2020-122
Preprint. Discussion started: 29 June 2020

JCGM: International Vocabulary of Metrology - Basic and General Concepts and Associated Terms, Tech. rep., Joint Committee for Guides in Metrology (JCGM), http://www.bipm.org/utils/common/documents/jcgm/JCGM_200_2012.pdf, 2012.

Joiner, J. and Vasilkov, A. P.: First results from the OMI rotational Raman scattering cloud pressure algorithm, IEEE Trans. Geosci. Remote Sens., 44, 1272–1282, 2006.

Keppens, A., Compernolle, S., Verhoelst, T., Hubert, D., and Lambert, J.-C.: Harmonization and comparison of vertically resolved atmospheric state observations: methods, effects, and uncertainty budget, Atmos. Meas. Tech., 12, 4379–4391, https://doi.org/10.5194/amt-12-4379-2019, 2019.

Koelemeijer, R. B. A., Stammes, P., Hovenier, J. W., and de Haan, J. F.: A fast method for retrieval of cloud parameters using oxygen A band measurements from the Global Ozone Monitoring Experiment, J. Geophys. Res., 106, 3475–3490, https://doi.org/10.1029/2002JD002429, 2001.

Lambert, J.-C., De Clercq, C., and von Clarmann, T.: Combining and merging water vapour observations: A multi-dimensional perspective on smoothing and sampling issues, in: Monitoring Atmospheric Water Vapour, edited by Kämpfer, N., vol. 10 of *ISSI Scientific Report Series*, chap. 10, pp. 215–242, Springer-Verlag New York, https://doi.org/10.1007/978-1-4614-3909-7, 2013.

Levelt, P. F., Joiner, J., Tamminen, J., Veefkind, J. P., Bhartia, P. K., Stein Zweers, D. C., Duncan, B. N., Streets, D. G., Eskes, H., van der A, R., McLinden, C., Fioletov, V., Carn, S., de Laat, J., DeLand, M., Marchenko, S., McPeters, R., Ziemke, J., Fu, D., Liu, X., Pickering, K., Apituley, A., González Abad, G., Arola, A., Boersma, F., Chan Miller, C., Chance, K., de Graaf, M., Hakkarainen, J., Hassinen, S., Ialongo, I., Kleipool, Q., Krotkov, N., Li, C., Lamsal, L., Newman, P., Nowlan, C., Suleiman, R., Tilstra, L. G., Torres, O., Wang, H., and Wargan, K.: The Ozone Monitoring Instrument: overview of 14 years in space, Atmos. Chem. Phys., 18, 5699–5745, https://doi.org/10.5194/acp-18-5699-2018, 2018.

Loew, A., Bell, W., Brocca, L., Bulgin, C. E., Burdanowitz, J., Calbet, X., Donner, R. V., Ghent, D., Gruber, A., Kaminski, T., Kinzel, J., Klepp, C., Lambert, J.-C., Schaepman-Strub, G., Schröder, M., and Verhoelst, T.: Validation practices for satellite-based Earth observation data across communities, Rev. Geophys., p. 779– 817, https://doi.org/10.1002/2017RG000562, 2017.

Loyola, D.: A new cloud recognition algorithm for optical sensors, in: Geoscience and Remote Sensing Symposium Proceedings, IGARSS '98. 1998 IEEE International, vol. 2, pp. 572–574, 1998.

Loyola, D. G., Thomas, W., Spurr, R., and Mayer, B.: Global patterns in daytime cloud properties derived from GOME backscatter UV-VIS measurements, Int. J. Remote. Sens., 31, 4295–4318, https://doi.org/10.1080/01431160903246741, 2010.

Loyola, D. G., Pedergnana, M., and Gimeno García, S.: Smart sampling and incremental function learning for very large high dimensional data, Neural Networks, 78, 75 – 87, https://doi.org/https://doi.org/10.1016/j.neunet.2015.09.001, special Issue on Neural Network Learning in Big Data, 2016.

Loyola, D. G., Gimeno García, S., Lutz, R., Argyrouli, A., Romahn, F., Spurr, R. J. D., Pedergnana, M., Doicu, A., Molina García, V., and Schüssler, O.: The operational cloud retrieval algorithms from TROPOMI on board Sentinel-5 Precursor, Atmos. Meas. Tech., 11, 409–427, https://doi.org/10.5194/amt-11-409-2018, 2018.

Loyola, D. G., Xu, J., Heue, K.-P., and Zimmer, W.: Applying FP_ILM to the retrieval of geometry-dependent effective Lambertian equivalent reflectivity (GE_LER) daily maps from UVN satellite measurements, Atmos. Meas. Tech., 13, 985–999, https://doi.org/10.5194/amt-13-985-2020, 2020.

Loyola, D. G. R.: Automatic cloud analysis from polar-orbiting satellites using neural network and data fusion techniques, in: IGARSS 2004. 2004 IEEE International Geoscience and Remote Sensing Symposium, vol. 4, pp. 2530–2533, 2004.

https://doi.org/10.5194/amt-2020-122
Preprint. Discussion started: 29 June 2020

Lutz, R., Loyola, D., Gimeno García, S., and Romahn, F.: OCRA radiometric cloud fractions for GOME-2 on MetOp-A/B, Atmos. Meas. Tech., 9, 2357–2379, https://doi.org/10.5194/amt-9-2357-2016, 2016.

McPeters, R. D., Bhartia, P. K., Haffner, D., Labow, G. J., and Flynn, L.: The version 8.6 SBUV ozone data record: An overview, J. Geophys. Res. Atmos., 118, 8032–8039, https://doi.org/doi:10.1002/jgrd.50597, 2013.

Molina García, V., Sasi, S., Efremenko, D. S., Doicu, A., and Loyola, D.: Radiative transfer models for retrieval of cloud parameters from EPIC/DSCOVR measurements, J. Quant. Spectrosc. Radiat. Transfer, 213, 228–240, https://doi.org/https://doi.org/10.1016/j.jqsrt.2018.03.014, 2018.

Nakajima, T. and King, M. D.: Determination of the Optical Thickness and Effective Particle Radius of Clouds from Reflected Solar Radiation Measurements. Part I: Theory, J. Atmos. Sci., 47, 1878–1893, https://doi.org/10.1175/1520-0469(1990)047<1878:DOTOTA>2.0.CO;2, https://doi.org/10.1175/1520-0469(1990)047<1878:DOTOTA>2.0.CO;2, 1990.

Platnick, S., Meyer, K. G., King, M. D., Wind, G., Amarasinghe, N., Marchant, B., Arnold, G. T., Zhang, Z., Hubanks, P. A., Holz, R. E., Yang, P., Ridgway, W. L., and Riedi, J.: The MODIS Cloud Optical and Microphysical Products: Collection 6 Updates and Examples From Terra and Aqua, IEEE Trans. Geosci. Remote Sens., 55, 502–525, https://doi.org/10.1109/TGRS.2016.2610522, 2017.

Platnick, S. et al.: MODIS Atmosphere L3 Daily Product. NASA MODIS Adaptive Processing System, Goddard Space Flight Center, USA, https://doi.org/10.5067/MODIS/MYD08_D3.061, 2015.

Platnick, S. et al.: VIIRS Atmosphere L2 Cloud Properties Product. Version-1. Goddard Space Flight Center, USA, https://doi.org/10.5067/VIIRS/CLDPROP_L2_VIIRS_SNPP.001, 2017.

Schiffer, R. A. and Rossow, W. B.: The International Satellite Cloud Climatology Project (ISCCP): The First Project of the World Climate Research Programme, Bull. Amer. Meteor. Soc., 64, 779–784, https://doi.org/10.1175/1520-0477-64.7.779, 1983.

Schuessler, O., Rodriguez, D. G. L., Doicu, A., and Spurr, R.: Information Content in the Oxygen A-Band for the Retrieval of Macrophysical Cloud Parameters, IEEE Trans. Geosci. Remote Sensing, 52, 3246–3255, https://doi.org/10.1109/tgrs.2013.2271986, 2014.

Siddans, R.: S5P-NPP Cloud Processor ATBD, Tech. Rep. S5P-NPPC-RAL-ATBD-0001, issue 1.0.0, 2016-02-12, Rutherford Appleton Laboratory (RAL), https://sentinels.copernicus.eu/documents/247904/2476257/Sentinel-5P-NPP-ATBD-NPP-Clouds, 2016.

Sneep, M., de Haan, J. F., Stammes, P., Wang, P., Vanbauce, C., Joiner, J., Vasilkov, A. P., and Levelt, P. F.: Three-way comparison between OMI and PARASOL cloud pressure products, J. Geophys. Res., 113, D15S23, https://doi.org/10.1029/2007jd008694, 2008.

Spurr, R. J.: VLIDORT: A linearized pseudo-spherical vector discrete ordinate radiative transfer code for forward model and retrieval studies in multilayer multiple scattering media, J. Quant. Spectrosc. Radiat. Transfer, 102, 316 – 342, https://doi.org/10.1016/j.jqsrt.2006.05.005, 2006.

Stammes, P., Sneep, M., de Haan, J. F., Veefkind, J. P., Wang, P., and Levelt, P. F.: Effective cloud fractions from the Ozone Monitoring Instrument: Theoretical framework and validation, J. Geophys. Res., 113, D16S38, https://doi.org/10.1029/2007jd008820, 2008.

Taylor, K. E.: Summarizing multiple aspects of model performance in a single diagram, J. Geophys. Res., 106, 7183–7192, https://doi.org/10.1029/2000jd900719, 2001.

Tilstra, L. G., Tuinder, O. N. E., Wang, P., and Stammes, P.: Surface reflectivity climatologies from UV to NIR determined from Earth observations by GOME-2 and SCIAMACHY, J. Geophys. Res., 122, 4084–4111, https://doi.org/10.1002/2016JD025940, 2017.

Veefkind, J., Acarreta, J., and Sneep, M. C.: OMI Level 2 O_2-O_2 Cloud Data Product Specification, Tech. Rep. SD-OMIE-KNMI-325, KNMI, 2009.

Veefkind, J., Aben, I., McMullan, K., Förster, H., de Vries, J., Otter, G., Claas, J., Eskes, H., de Haan, J., Kleipool, Q., van Weele, M., Hasekamp, O., Hoogeveen, R., Landgraf, J., Snel, R., Tol, P., Ingmann, P., Voors, R., Kruizinga, B., Vink, R., Visser, H., and Levelt, P.:

https://doi.org/10.5194/amt-2020-122
Preprint. Discussion started: 29 June 2020

TROPOMI on the ESA Sentinel-5 Precursor: A GMES mission for global observations of the atmospheric composition for climate, air quality and ozone layer applications, Remote Sens. Environ., 120, 70–83, https://doi.org/10.1016/j.rse.2011.09.027, 2012.

Veefkind, J. P., de Haan, J. F., Sneep, M., and Levelt, P. F.: Improvements to the OMI O_2-O_2 operational cloud algorithm and comparisons with ground-based radar-lidar observations, Atmos. Meas. Tech., 9, 6035–6049, https://doi.org/10.5194/amt-9-6035-2016, 2016.

Verhoelst, T. and Lambert, J. C.: Generic metrology aspects of an atmospheric composition measurement and of data comparisons. EC Horizon2020 GAIA-CLIM technical Report / Deliverable D3.2, Tech. rep., BIRA-IASB, http://www.gaia-clim.eu/system/files/publications, 2016.

Verhoelst, T., Granville, J., Hendrick, F., Köhler, U., Lerot, C., Pommereau, J.-P., Redondas, A., Van Roozendael, M., and Lambert, J.-C.: Metrology of ground-based satellite validation: co-location mismatch and smoothing issues of total ozone comparisons, Atmos. Meas. Tech., 8, 5039–5062, https://doi.org/10.5194/amt-8-5039-2015, 2015.

Wang, P. and Stammes, P.: Evaluation of SCIAMACHY Oxygen A band cloud heights using Cloudnet measurements, Atmos. Meas. Tech., 7, 1331–1350, https://doi.org/10.5194/amt-7-1331-2014, 2014.

Wang, P., Stammes, P., R., v., Pinardi, G., and van Roozendael, M.: FRESCO+: an improved O_2 A-band cloud retrieval algorithm for tropospheric trace gas retrievals, Atmos. Chem. Phys., 8, 6565–6576, https://doi.org/10.5194/acp-8-6565-2008, 2008.

Wang, P., Tuinder, O. N. E., and Stammes, P.: FRESCO+ v2 for GOME-2 L1b PPF, ATBD. Final report of EUM/CO/09/4600000655/RM., Tech. rep., EUMETSAT, https://www.eumetsat.int/website/home/Data/TechnicalDocuments/index.html, 2016.

Zeng, S., Cornet, C., Parol, F., Riedi, J., and Thieuleux, F.: A better understanding of cloud optical thickness derived from the passive sensors MODIS/AQUA and POLDER/PARASOL in the A-Train constellation, Atmos. Chem. Phys., 12, 11 245–11 259, https://doi.org/10.5194/acp-12-11245-2012, 2012.